

# Form factors of light pseudoscalar mesons from the perturbative QCD approach

---

Jian Chai<sup>a,b</sup> and Shan Cheng<sup>b,c,d</sup> <sup>1</sup>

<sup>a</sup>*Institute of Theoretical Physics, School of Sciences, Henan University of Technology, Zhengzhou, Henan 450001, China*

<sup>b</sup>*School of Physics and Electronics, Hunan University, 410082 Changsha, China*

<sup>c</sup>*School for Theoretical Physics, Hunan University, 410082 Changsha, China*

<sup>d</sup>*Hunan Provincial Key Laboratory of High-Energy Scale Physics and Applications, 410082 Changsha, China*

*E-mail:* [scheng@hnu.edu.cn](mailto:scheng@hnu.edu.cn)

**ABSTRACT:** We study the electromagnetic and meson-photon transition form factors of light pseudoscalar mesons from the perturbative QCD (pQCD) approach. In order to include the soft transversal degree of freedom of partons inside hadrons, we introduce the intrinsic transversal momentum distributions (iTMDs), accompanying to the light-cone distribution amplitudes (LCDAs) which depict the longitudinal nonperturbative dynamics of an energetic meson. The main motivations of this work are the disjointedness of electromagnetic form factors between the theoretical predictions and the experimental measurements, and the BABAR-Belle tension of pion-photon transition form factor in the large momentum transfers. Our calculation is carried out at the next-to-leading-order for the contributions from leading and subleading twist LCDAs, and leading order for the twist four contributions. For the meson-photon transition form factors, the high twist contributions are considered as the first time. The main result of this paper are (a) the iTMDs play an important role to explain the data of form factors, especially in the small and intermediate momentum transfers where the pQCD prediction is decreased sizable in the magnitude, (b) the transversal-size parameters of pion and kaon mesons associated to the valence quark state are  $\beta_\pi^2 = 0.51 \pm 0.04 \text{ GeV}^{-2}$  and  $\beta_K^2 = 0.30 \pm 0.05 \text{ GeV}^{-2}$ , the chiral mass of pion meson is  $m_0^\pi(1 \text{ GeV}) = 1.84 \pm 0.07 \text{ GeV}$ , (c) the meson-photon TFFs are dominated by the leading twist LCDAs, the iTMDs-improved pQCD calculations favor the Belle data of pion TFF in the intermediate and large momentum transfers, and prefer a small mixing angle between  $\eta$  and  $\eta'$ , (d) impressively, the inclusion of iTMDs improves the pQCD prediction down to a few  $\text{GeV}^2$  for all the form factors discussed in this paper.

---

<sup>1</sup>Corresponding author.

---

## Contents

<b>1</b>	<b>Introduction</b>	<b>1</b>
<b>2</b>	<b>Electromagnetic form factors</b>	<b>3</b>
2.1	Intrinsic transversal momentum distribution functions	7
2.2	Electromagnetic form factor of pion	10
2.3	Electromagnetic form factor of kaon	14
<b>3</b>	<b>Meson-Photon transition form factors</b>	<b>19</b>
3.1	pQCD formulism	22
3.2	Transition form factor of pion	24
3.3	Transition form factor of $\eta, \eta'$ mesons	25
<b>4</b>	<b>Summary</b>	<b>30</b>
<b>5</b>	<b>ACKNOWLEDGEMENTS</b>	<b>31</b>
<b>A</b>	<b>Definition of the light-cone distribution amplitudes</b>	<b>32</b>
<b>B</b>	<b>Expressions of the light-cone distribution amplitudes</b>	<b>33</b>
<b>C</b>	<b>A Derivation of the modulus squared dispersion relation</b>	<b>35</b>

---

## 1 Introduction

Emergence occurs when an entity is observed to have properties its parts do not have on their own, properties or behaviors which emerge only when the parts interact in a wider whole. In this sense, confinement is a emergent phenomena in QCD which states that the physical states are color singlets with internal quark and gluon degrees of freedom. This is the basic idea of the parton picture to understand the hadron structures [1, 2] and the factorization theorem to separate the contributions of small and large distances in hadron amplitudes [3, 4].

People have introduced several types of functions to describe the parton distributions inside a hadron. The most simplest one is the one-dimension parton distribution amplitudes (PDF) which is a function of longitudinal momentum fraction  $x_i$ . In order to consider the transversal momentum distribution in the small  $x$  physics, people defined the transversal momentum dependent distribution amplitudes (TMD) and also its transversal conjugated function, saying the generalized parton distributions (GPD) [5, 6]. The above

functions are introduced to deal with the inclusive processes mainly happened in the fixed target experiments like Jefferson Laboratory and EIC. For the exclusive processes happened in the collider experiments with large momentum transfers, people introduce the light-cone distribution amplitudes (LCDAs), which provides a rigorous twist (power) expansion of the parton distribution in the infinity momentum frame.

To our knowledge, the first systematic high twist analysis of hadron LCDAs is studied for the pion in connection with the problem of possible corrections to the pion form factors [7], the study is then extended to the  $K$  meson with including the structure of  $SU(3)$ -breaking corrections [8], the vector mesons [9–12] and the nucleons [13]. With the unique advantage of rigorous power expansion, the LCDAs description is widely used in the hard exclusive QCD processes. Taking the pion as an example, based on the in-depth understanding of the leading twist LCDAs, people have promoted the QCD calculation of the transition form factor [14–16] up to the next-to-next-to-leading-order (NNLO) [17, 18]. The high precise calculation of photon-pion transition reduces the hadronic uncertainties in explaining the  $g-2$  anomaly [19]. In addition, the electromagnetic pion form factor [20–28] and the  $B \rightarrow \pi$  form factors are also calculated to the next-to-leading-order (NLO) at subleading twist level of pion LCDAs [29–33].

In contrast to the more and more precise hard amplitudes from the perturbative QCD calculation, the nonperturbative LCDAs are not well understood yet. Generally speaking, there are three different ways to study the shape of LCDAs. They are the nonperturbative QCD approaches like the sum rules (QCDSRs) and the instanton vacuum model, the lattice QCD (LQCD) evaluation from the claimed first-principle, as well as the data-driven method. Starting from the appropriate correlation functions, the QCDSR is able to predict the lowest gegenbauer expansion coefficient of leading twist LCDAs, However, it is powerless for the higher coefficients due to the nonlocal vacuum condensates introduced with large model dependence. For the higher gegenbauer coefficients, the LQCD encounters high-order differentiation and results to a poor signal-to-noise ratio. The last but not the least, people can determine the higher coefficients from the data-driven method by fitting the theoretical predictions to the measurements. But keep in mind that it firstly requires both the precise calculation and measurement as the inputs, in addition, the fit is truncated to a certain term with the ansatz that the gegenbauer expansion is convergent.

In this paper, we focus on the light pseudoscalar mesons, trying to understand their fine structures by answer three questions. The first one is the mismatch between QCD-based predictions and the direct measurement of electromagnetic form factors (EMFFs). The QCD predictions are usually powerful in the intermediate and large Euclidean moment space with negative  $q^2$ , while the available data are reliable in the small spacelike region and in the physical timelike regions. This mismatch in sharp reduces the power of data-driven method to extract LCDAs. Secondly, the rapid-increasing pion-photon transition form factors (TFFs) in the large momentum transfers reported by the BaBar collaboration was not confirmed by the Belle collaboration. Besides the BESIII measurement in the  $\rho - \omega$  region, there is no further measurements in the last decade. From the theoretical

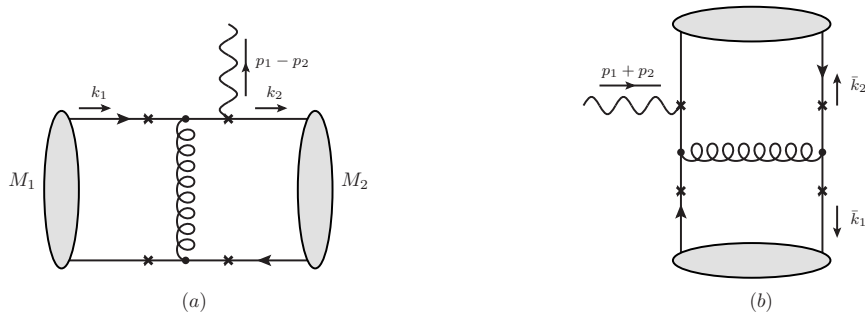


**Figure 1.** Feynman diagrams of EMFFs at leading order, here "  $\times$  " denotes the possible electromagnetic interaction vertexes.

side, this process is very sensitive to the leading twist LCDAs of pion meson, and hence it is a benchmark process to understand the goldstone pion meson. the last but not the least, the difference of  $\eta$  and  $\eta'$  TFFs measured in the low and intermediate momentum transfers provides an opportunity to examine the mixing scheme of isoscalar contents  $\eta_1$ ,  $\eta_8$  and  $\eta_c$ .

The paper is arranged as follow. In the next section 2, the dispersion relations are introduced in the modular representation to built the relation between timelike and space-like EMFFs in a model independent way, the feasible data-driven study of pion and kaon mesons are presented subsequently. In Section 3, the photon-pion TFF is well-treated in the pQCD approach with the LCDAs and the intrinsic transversal momentum distribution function extracted in section 2. We then study the TFFs of isoscalar light pseudoscalar mesons  $\eta$ ,  $\eta'$ , trying to understand the measurements under different mixing schemes. The summary is given in Section 4.

## 2 Electromagnetic form factors

As the most simplest hadronic matrix element, form factors play a crucial role to examine the factorization theorem and perturbative QCD calculation if one knows the hadron structures well. Conversely, it could help us to understand the dynamical structure of hadrons with the high precise QCD calculation. There are two types form factors appeared in the hard exclusive QCD processes. For the heavy-to-light transitions, the smallness of interaction distance in the perturbative calculation is guaranteed by the internal reason, saying the heavy mass of  $W/Z$  bosons and heavy quarks. In contrast, the small interaction distance in the electromagnetic and meson-photon transitions is guaranteed by the external large momentum transfers. In this paper, we focus on the latter ones, trying to understand the fine structures of light pseudoscalar mesons from the state-of-the-art perturbative calculations and the precise experiment measurements.

In this section we discuss the EMFFs of pion and kaon mesons, they describe the possibility to be happened when a hadron is kicked by an energetic photon while not been broken down. In the view of perturbative QCD, the energetic photon changes the momentum of the interacted parton significantly, a hard gluon is hence required to exchange

momentum between the interacted and the spectator partons to form the final meson. We depict the leading order (LO) feynman diagrams of the spacelike (left) and timelike (right) form factors in figure 1. They are defined by the matrix elements sandwiched by a electromagnetic current  $j_\mu^{\text{em}} = e_u \bar{u} \gamma_\mu u + e_d \bar{d} \gamma_\mu d + e_s \bar{s} \gamma_\mu s$ , here  $e_q$  denotes the fractional charge quark participated in the interaction. For the charged pseudoscalar mesons ( $\mathcal{P} = \pi, K$ ), it is defined by

$$\begin{aligned} \langle \mathcal{P}^+(p_2) | J_\mu^{\text{em}} | \mathcal{P}^+(p_1) \rangle &= e_q (p_1 + p_2)_\mu \mathcal{F}_\mathcal{P}(Q^2), \\ \langle \mathcal{P}^+(p_2) \mathcal{P}^-(p_1) | J_\mu^{\text{em}} | 0 \rangle &= e_q (p_1 - p_2)_\mu \mathcal{G}_\mathcal{P}(Q^2). \end{aligned} \quad (2.1)$$

In the QCD processes with large momentum transfers, one can treat the quark lines with large virtuality as free propagators. This means to keep only the large fourier components of the nonlocal quark operators and omit the nonperturbative effects appeared as power corrections, like  $\langle 0 | G_{\mu\nu}^2 | 0 \rangle / q^4$ . Meanwhile, the lines with small virtuality are retained in the Heisenberg operator. This is the string operator representation of the factorization idea, which provides an effective covariant technique to separate the contributions of small and large distances in a physical amplitude.

The electromagnetic matrix element is then written in a factorization formula as

$$\begin{aligned} &\langle \mathcal{P}(p_2) | J_\mu^{\text{em}} | \mathcal{P}(p_1) \rangle \\ &= \oint dz_1 dz_2 \langle \mathcal{P}(p_2) | \left\{ \bar{q}_{1\gamma}(0) \exp \left( i g_s \int_{z_2}^0 d\sigma_\nu A^\nu(\sigma) \right) q_{2\beta}(z_2) \right\}_{kj} | 0 \rangle_{\mu_t} \\ &\cdot H_{\gamma\beta\alpha\delta}^{ijkl}(z_1, 0) \langle 0 | \left\{ \bar{q}_{2\alpha}(z_2) \exp \left( i g_s \int_{z_1}^{z_2} d\sigma_\nu A^\nu(\sigma) \right) q_{1\delta}(z_1) \right\}_{il} | \mathcal{P}(p_1) \rangle_{\mu_t}, \end{aligned} \quad (2.2)$$

where  $\gamma, \beta, \alpha, \delta$  are the spinor indices, and  $i, j, k, l$  are the color indicators. The hard kernel associated with the lowest Fock state is

$$H_{\gamma\beta\alpha\delta}^{ijkl}(z_1, z_2) = -i [g_s \gamma_m]_{\alpha\beta} T^{ij} [(e_q \gamma_\mu) S^{(0)}(z_2 - z_1) (g_s \gamma_n)]_{\gamma\delta} T^{kl} D_{mn}^{(0)}(z_2 - z_1). \quad (2.3)$$

Here the quark and gluon free propagators read as

$$S^{(0)}(z) = \frac{1}{2\pi^2} \frac{\not{z}}{z^4}, \quad D_{mn}^{(0)}(z) = \frac{1}{4\pi^2} \frac{g_{mn}}{z^2}. \quad (2.4)$$

The nonlocal matrix elements in the RHS of Eq. (2.2) imply the amplitudes of mesons breaking-up into a pair of soft quarks, they receive contributions from different lorentz structures

$$4\bar{q}_{1\alpha} q_{2\delta} = \left\{ \bar{q}_1 q_2 + \gamma_5 (\bar{q}_2 \gamma_5 q_1) + \gamma^\rho (\bar{q}_2 \gamma_\rho q_1) + \gamma_5 \gamma^\rho (\bar{q}_1 \gamma_\rho \gamma_5 q_1) + \frac{\sigma^{\rho\tau}}{2} (\bar{q}_2 \sigma_{\rho\tau} q_1) \right\}_{\delta\alpha} \quad (2.5)$$

and define the light cone distribution amplitudes (LCDAs) of meson at different twists. The details of LCDAs definition are presented in appendix A.

The state-of-the-art perturbative QCD (pQCD) predictions of EMFFs are written as

$$\mathcal{F}_{\mathcal{P}}^{\text{em}}(Q^2) = \mathcal{F}_{\mathcal{P}}^{2p}(Q^2) + \mathcal{F}_{\mathcal{P}}^{3p}(Q^2) \quad (2.6)$$

$$\begin{aligned} \mathcal{F}_{\mathcal{P}}^{2p}(Q^2) = & \frac{8}{9}\pi\alpha_s f_{\mathcal{P}}^2 Q^2 \int_0^1 du_1 \int_0^1 du_2 \int_0^{1/\Lambda} b_1 db_1 b_2 db_2 e^{-S(x_i, y_i, b_1, b_2, \mu)} \\ & \cdot S_t(u_1, t) S_t(u_2, t) \left\{ u_2 \varphi(u_1) \varphi(u_2) \left( 1 + F_{t2}^{(1)}(u_1, u_2, t, Q^2) \right) \mathcal{H} \right. \\ & + \frac{2m_0^2}{Q^2} \left[ (1 - u_2) \varphi^p(u_1) \varphi^p(u_2) \left( 1 + F_{t3}^{(1)}(u_1, u_2, t, Q^2) \right) \mathcal{H}_0 \right. \\ & + \frac{1}{3} \varphi^p(u_1) \varphi^\sigma(u_2) \left( 1 + \tilde{F}_{t3}^{(1)}(u_1, u_2, t, Q^2) \right) \\ & \cdot \left. \left. \left( \mathcal{H}_0 - (1 - u_2) Q^2 \mathcal{H}_1 - u_2 (1 + u_1) \mathcal{H}_2 \right) \right] \right. \\ & - \left[ 2 (u_2)^2 \phi(u_1) g_2(u_2) - 4 u_2 \phi(u_1) (g_1(u_2) + \tilde{g}_2(u_2)) \right] \mathcal{H}_1 \\ & - \left[ 2 u_1 u_2 \phi(u_2) g_2(u_1) + 4 u_2 \phi(u_1) (g_1(u_2) + \tilde{g}_2(u_2)) \right] \mathcal{H}_2 \\ & + \left[ 4 (u_2)^2 (1 + u_1) Q^2 \phi(u_1) (g_1(u_2) + \tilde{g}_2(u_2)) \right] \mathcal{H}_3 \left. \right\}, \quad (2.7) \end{aligned}$$

$$\begin{aligned} \mathcal{F}_{\mathcal{P}}^{3p}(Q^2) = & \frac{64}{9}\pi\alpha_s f_{\mathcal{P}}^2 Q^2 \int_0^1 \mathcal{D}u_{1i} \int_0^1 \mathcal{D}u_{2i} \int_0^{1/\Lambda} b_1 db_1 b_2 db_2 e^{-S^3(u_{1i}, u_{2i}, b_1, b_2, \mu)} \\ & S_t(u_{1i}, Q) S_t(u_{2i}, Q) \tilde{\varphi}_{\parallel}(u_{2i}) \varphi_{\parallel}(u_{1i}) v \bar{v} \\ & \cdot \left\{ \mathcal{H}'_0 + u_{22} Q^2 \mathcal{H}'_1 - [3 u_{11} u_{22} (u_{11} + u_{21} + u_{11} u_{22}) Q^4] \mathcal{H}'_2 \right\}. \quad (2.8) \end{aligned}$$

The contribution from two-particle and three-particle LCDAs are written separately. Here we show explicitly the result of spacelike form factor with  $Q^2 = -q^2 = -(p_1 + p_2)^2$ , the result of timelike form factors can be obtained by a simple kinematical replacement  $-Q^2 \rightarrow Q^2$ .

In the pQCD equations (2.7,2.8),  $f_{\mathcal{P}}$  is the decay constant defined via the local matrix element

$$\langle 0 | \bar{q}_1 \gamma_\mu \gamma_5 q_2 | \mathcal{P}(p) \rangle = i f_{\mathcal{P}} p_\mu. \quad (2.9)$$

$\phi$ ,  $\phi^{p,\sigma}$  and  $g_{1,2}$  are the leading twist, twist three and twist four LCDAs associated to valence quark state ( $\bar{q}_1 q_2$ ) of  $\mathcal{P}$  meson, and  $\varphi_{\parallel}$  is the twist four LCDAs associated to the three-particle state ( $\bar{q}_1 q_2 g$ ). The auxiliary LCDAs

$$\tilde{g}_2(u_2) \equiv \int_0^{u_2} du'_2 g_2(u'_2), \quad \tilde{\varphi}_{\parallel}(u_{2i}) \equiv \int_0^{u_{22}} du'_{22} \varphi_{\parallel}(u'_{2i}) \quad (2.10)$$

satisfy the bound conditions  $\tilde{g}_2(u_2 = 0, 1) = 0$  and  $\tilde{\varphi}_{\parallel}(u_{22} = 0, 1) = 0$ . In the LCDAs functions,  $u_1$  and  $u_2$  are the longitudinal momentum fractions in the two-particle LCDAs carried by the anti-quark in the initial meson and the quark in the final meson,  $u_{1i}$  and  $u_{2i}$  are the momentum fractions of partons in the three-particle LCDAs in which  $i = 1, 2, 3$  corresponding to antiquarks, quarks and gluons, respectively. The momentum fractions of

gluons are absorbed effectively into the momentum fraction of antiquark with the weighted parameter and the measure of path-integral

$$v \equiv \frac{u_1 - u_{11}}{1 - u_{11} - u_{12}}, \quad \int_0^1 \mathcal{D}u_{1i} \equiv \int_0^1 du_1 \int_0^{u_1} du_{11} \int_0^{1-u_1} \frac{du_{12}}{1 - u_{11} - u_{12}}. \quad (2.11)$$

$b_1$  and  $b_2$  are the conjugated coordinates to the transversal momenta associated to the internal quark propagators.

The transversal momentum  $k_T$  is picked up in the pQCD calculation to regulate the end-point singularity in the hard kernels. Generally speaking, it varies within three scales, saying the QCD scale  $\lambda$ , the hard-collinear scale  $\sqrt{\Lambda Q}$  and the hard scale  $Q$ . The loop integral of  $k_T$  results in several large logarithms, especially in the integral regions  $k_T \sim \Lambda$ . These logarithms are resummed up to the well-known sudakov factors  $S$  and  $S^3$ , which turns out to highly suppresses the soft contribution, meanwhile, highlight the hard scattering mechanism. The functions  $F_{t2}^{(1)}$  and  $F_{t3}^{(1)}$  appear in equations (2.6,2.7,2.8) are the next-to-leading-order (NLO) QCD corrections associated to the hard scattering amplitudes proportional to leading twist and twist three LCDAs, respectively [23–26]. Hard functions  $\mathcal{H}_{(i)}$  are written by means of the modified Bessel functions.

$$\begin{aligned} \mathcal{H}_0 &= K_0(\beta b_1) \left[ \theta(b_1 - b_2) I_0(\alpha b_2) K_0(\alpha b_1) - \theta(b_2 - b_1) I_0(\alpha b_1) K_0(\alpha b_2) \right], \\ \mathcal{H}_1 &= K_0(\beta b_1) \left[ \theta(b_1 - b_2) \left( \frac{b_1}{2\alpha} I_0(\alpha b_2) K_1(\alpha b_1) - \frac{b_2}{2\alpha} I_1(\alpha b_2) K_0(\alpha b_1) \right) \right. \\ &\quad \left. - \{b_1 \leftrightarrow b_2\} \right], \\ \mathcal{H}_2 &= \frac{b_1 K_1(\beta b_1)}{2\beta} \left[ \theta(b_1 - b_2) I_0(\alpha b_2) K_0(\alpha b_1) - \theta(b_2 - b_1) I_0(\alpha b_1) K_0(\alpha b_2) \right], \\ \mathcal{H}_3 &= \frac{b_1 K_1(\beta b_1)}{2\beta} \left[ \theta(b_1 - b_2) \left( \frac{b_1}{2\alpha} I_0(\alpha b_2) K_1(\alpha b_1) - \frac{b_2}{2\alpha} I_1(\alpha b_2) K_0(\alpha b_1) \right) \right. \\ &\quad \left. - \{b_1 \leftrightarrow b_2\} \right], \\ \mathcal{H}'_0 &= \frac{(b_1)^2 K_2(\beta' b_1)}{8(\beta')^2} \left[ \theta(b_1 - b_2) I_0(\alpha' b_2) K_0(\alpha' b_1) - \theta(b_2 - b_1) I_0(\alpha' b_1) K_0(\alpha' b_2) \right], \\ \mathcal{H}'_1 &= \frac{(b_1)^2 K_2(\beta' b_1)}{8(\beta')^2} \left[ \theta(b_1 - b_2) \left( \frac{b_1}{2\alpha} I_0(\alpha' b_2) K_1(\alpha' b_1) - \frac{b_2}{2\alpha} I_1(\alpha' b_2) K_0(\alpha' b_1) \right) \right. \\ &\quad \left. - \{b_1 \leftrightarrow b_2\} \right], \\ \mathcal{H}'_2 &= \frac{1}{48} \left[ \frac{(b_1)^3}{(\beta')^3} K_3(\beta' b_1) + \frac{b_1}{(\beta')^5} K_1(\beta' b_1) \right] \left[ \theta(b_1 - b_2) \right. \\ &\quad \left. \cdot \left( \frac{b_1}{2\alpha} I_0(\alpha' b_2) K_1(\alpha' b_1) - \frac{b_2}{2\alpha} I_1(\alpha' b_2) K_0(\alpha' b_1) \right) - \{b_1 \leftrightarrow b_2\} \right]. \end{aligned} \quad (2.12)$$

The hard scales appeared in the internal propagators read

$$\begin{aligned}\alpha &= [u_2 Q^2]^{1/2}, & \beta &= [u_1 u_2 Q^2]^{1/2}, \\ \alpha' &= [(u_{21} + u_{23}) Q^2]^{1/2}, & \beta' &= [u_{11} u_{21} Q^2]^{1/2}.\end{aligned}\quad (2.13)$$

We mark that the result in equations (2.7,2.8) shows some differences in contrast to the previous pQCD study [27]. The difference appears for the terms proportional to twist four LCDAs and the contributions from three-particle state, which are power suppressed by the transversal momentum  $\mathcal{O}(k_T^2/Q^2)$  and/or quark mass. The underlying dynamics of the discrepancy is the different treatments of the hard amplitudes in the pQCD calculations. Here we start with the string operator representation of the factorization idea in coordinate space, and transform it to the momentum space by integrating over the light-like coordinates. In the previous work [27], however, the hard amplitudes are calculated directly by feynman rules in the momentum space, the transversal terms on the numerators are hence not fully considered.

## 2.1 Intrinsic transversal momentum distribution functions

The renormalization scale of nonperturbative LCDAs is chosen as the same as the factorization one, which are taken at the largest virtuality in the scattering, saying  $\mu = \max(\sqrt{u_2}Q, 1/b_1, 1/b_2)$ . So roughly speaking, a LCDA embodied in the pQCD equations (2.7,2.8) is the wave function at zero transverse separations, this means that the soft transversal dynamics is actually missed in LCDAs [34, 35]. In order to include the soft transversal degree of freedom in the parton distribution of hadrons, we introduce the intrinsic transversal momentum distribution functions (iTMDs), supplementing to the LCDAs.

Soft pion wave function of the valence quark state  $\psi(u, \mathbf{k}_T)$  satisfies the normalization condition

$$\int \frac{du d^2 \mathbf{k}_T}{16\pi^3} |\psi(u, \mathbf{k}_T)|^2 = P_{q_1 \bar{q}_2} \leq 1. \quad (2.14)$$

Integrating over the transversal momenta, it deduces to the light-cone distribution amplitudes

$$\frac{f_{\mathcal{P}}}{2\sqrt{6}} \varphi(u, \mu) \equiv \int \frac{d^2 k_{\perp}}{16\pi^3} \psi(u, \mathbf{k}_T) \quad (2.15)$$

with satisfying the normalization conditions  $\int_0^1 du \varphi(u, \mu) = 1$ . This definition is self-consistent with the  $\pi \rightarrow \mu\nu$  decay [36] that

$$\frac{f_{\pi}}{2\sqrt{6}} = \int \frac{du d^2 k_{\perp}}{16\pi^3} \psi(u, \mathbf{k}_T). \quad (2.16)$$

$\psi(u, \mathbf{k}_T)$  is generally written by a product of LCDA and iTMDs,

$$\psi(u, \mathbf{k}_T) = \frac{f_{\mathcal{P}}}{2\sqrt{6}} \varphi(u, \mu) \Sigma(u, \mathbf{k}_T), \quad (2.17)$$



in which the transversal function itself should satisfies the normalization

$$\int \frac{d^2 k_\perp}{16\pi^3} \Sigma(u, \mathbf{k}_T) = 1. \quad (2.18)$$

We take the simple gaussian function of the  $k_T$  dependence wave function [37, 38]

$$\Sigma(u, \mathbf{k}_T) = 16\pi^2 \beta^2 g(u) \text{Exp} [-\beta^2 k_T^2 g(u)] \quad (2.19)$$

with  $g(u) = 1/(u\bar{u})$  retaining the rotational invariance. This expression is obtained from a harmonic oscillator in both the rest frame and the infinite momentum frame. The fourier transformation of the soft transversal wave function reads as

$$\hat{\Sigma}(u, \mathbf{b}_T) = 4\pi \text{Exp} \left[ -\frac{b_T^2 u(1-u)}{4\beta^2} \right], \quad (2.20)$$

the soft wave function defined in Eq. (2.17) is then modified to

$$\psi(u, \mathbf{b}_T) = \frac{f_\pi}{2\sqrt{6}} \varphi(u, \mu) \hat{\Sigma}(u, \mathbf{b}_T). \quad (2.21)$$

The transversal radius of the valence quark state should be smaller than (or at least equal to) the mean square electron charge radius of the pion  $\langle r_\pi^2 \rangle = 0.452 \pm 0.011 \text{ fm}^2$  [39]. In terms of the transversal momentum, it is replaced by a lower limit on the mean transversal momentum

$$[\langle \mathbf{k}_T^2 \rangle]^{1/2} = \left[ \frac{\int du d^2 \mathbf{k}_T \mathbf{k}_T^2 |\psi(u, \mathbf{k}_T)|^2}{\int du d^2 \mathbf{k}_T |\psi(u, \mathbf{k}_T)|^2} \right]^{1/2} \geq 300 \text{ MeV}. \quad (2.22)$$

It is argued that the double photon transition [35, 36] gives another constraint on the transversal-size parameter  $\beta_\pi^2$ , saying  $\int du \psi(u, \mathbf{k}_T = \mathbf{0}) = \sqrt{6}/f_\pi$ , which is written in terms of the gegenbauer coefficients

$$\beta_\pi^2 = \frac{1}{8\pi^2 f_\pi^2 (1 + a_2^\pi + a_4^\pi + \dots)}. \quad (2.23)$$

With the coefficients  $a_2^\pi(1\text{GeV}) = 0.28 \pm 0.05$ ,  $a_4^\pi(1\text{GeV}) = 0.19 \pm 0.06$  extracted recently from the electromagnetic form factor [22], and the decay constant  $f_\pi = 0.13 \text{ GeV}$  [39], we obtain  $\beta_\pi^2 = 0.511_{-0.035}^{+0.040} \text{ GeV}^{-2}$ . This value corresponds to the mean transversal momentum  $[\langle \mathbf{k}_T^2 \rangle]^{1/2} = 358 \pm 15 \text{ MeV}$ , satisfying the Eq. (2.22).

As shown in equations (B.2-B.4), there are three sources for the high (power) twist LCDAs. They are the "bad" components with "wrong" spin projection in the wave functions, the transversal motion of valence quark Fock state in the leading twist components, and the higher Fock states with an additional gluon or quark-antiquark pair. The first two are defined to the genuine two-particle twist three LCDAs and their scale evolutions, the third one gives the quark mass correction terms in the two-particle twist three LCDAs. Note that the second source is partially related to the third one by the equation of motion.

We also note that the transversal motion in the high twist LCDAs is definitely independent of the iTMDs introduced in this work, since they transfer different dynamics (hard/hard-collinear and soft) in the factorization formula.

We rewrite twist three LCDAs in a compact form to distinguish the contribution from the valence quark state and the three-particle state.

$$\varphi^{p,\sigma}(u, \mu) = \varphi_{2p}^{p,\sigma}(u, \mu) + \varphi_{3p}^{p,\sigma}(u, \mu). \quad (2.24)$$

in which the three-particle terms are furtherly decomposed to

$$\varphi_{3p}^{p,\sigma}(u, \mu) = \rho_{\pm} \varphi_{\text{EOM}}^{p,\sigma}(u, \mu) + \eta_3 \varphi_{qqg}^{p,\sigma}(u, \mu). \quad (2.25)$$

Here  $\rho_{\pm} \equiv \frac{m_{q_1 \pm m_{q_2}}}{m_0}$ , and  $\eta_3$  is a three-particle parameter.

The soft transversal function accompanied with the valence quark state is written in Eq. (2.19) and Eq. (2.20). For the soft transversal function associated to three-particle state, we propose another iTMD function  $\Sigma'$ .

$$\begin{aligned} \frac{f_{\pi} m_0^P}{2\sqrt{6}} \varphi^{p,\sigma}(u, \mu) &= \int \frac{d^2 \vec{k}_T}{16\pi^3} \varphi_{2p}^{p,\sigma}(u, \mathbf{k}_T) + \int \frac{d^2 \mathbf{k}_{1T} d^2 \mathbf{k}_{2T}}{16\pi^3 4\pi^2} \rho_{\pm} \varphi_{3p}^{p,\sigma}(u, \mathbf{k}_{1T}, \mathbf{k}_{2T}). \\ \psi_{2p}^{p,\sigma}(u, \mathbf{k}_T) &= \frac{f_{\pi} m_0^P}{2\sqrt{6}} \varphi_{2p}^{p,\sigma}(u, \mu) \Sigma(u, \mathbf{k}_T), \\ \psi_{3p}^{p,\sigma}(u, \mathbf{k}_{1T}, \mathbf{k}_{2T}) &= \frac{f_{\pi} m_0^P}{2\sqrt{6}} \varphi_{3p}^{p,\sigma}(u, \mu) \int_0^u d\alpha_1 \int_0^{\bar{u}} d\alpha_2 \frac{\Sigma'(\alpha_i, \mathbf{k}_{1T}, \mathbf{k}_{2T})}{1 - \alpha_1 - \alpha_2}. \end{aligned} \quad (2.26)$$

The normalization  $\int_0^1 du \varphi^p(u) = 1$  is then guaranteed by the normalizations of the iTMDs

$$\begin{aligned} \int \frac{d^2 k_{\perp}}{16\pi^3} \Sigma(u, \mathbf{k}_T) &= 1, \quad \int_0^u d\alpha_1 \int_0^{\bar{u}} d\alpha_2 \int \frac{d^2 \mathbf{k}_{1T} d^2 \mathbf{k}_{2T}}{16\pi^3 4\pi^2} \frac{\Sigma'(\alpha_i, \mathbf{k}_{1T}, \mathbf{k}_{2T})}{1 - \alpha_1 - \alpha_2} = 1, \\ \int_0^1 du \varphi_{2p}^{p,\sigma}(u, \mu) &= 1, \quad \int_0^1 du \varphi_{3p}^{p,\sigma}(u, \mu) = 0. \end{aligned} \quad (2.27)$$

The new introduced iTMD function is chosen again in a harmonic oscillator expression

$$\Sigma'(\alpha_i, \mathbf{k}_{1T}, \mathbf{k}_{2T}) = \frac{64\pi^3 \beta'^4}{\alpha_1 \alpha_2 (1 - \alpha_1 - \alpha_2)} \text{Exp} \left[ -\beta'^2 \left( \frac{k_{1T}^2}{\alpha_1} + \frac{k_{2T}^2}{\alpha_2} + \frac{(k_{1T} + k_{2T})^2}{1 - \alpha_1 - \alpha_2} \right) \right] \quad (2.28)$$

The fourier transformation leads to the faussian function in terms of transversal distance.

$$\hat{\Sigma}'(\alpha_i, \mathbf{b}_1, \mathbf{b}_2) = 4\pi \text{Exp} \left[ -\frac{2\alpha_3(b_1^2 + b_2^2) + (\alpha_1 + \alpha_2)(b_1 - b_2)^2}{16\beta'^2} \right]. \quad (2.29)$$

We notice that the crossing symmetry between  $\alpha_1$  and  $\alpha_2$  is took into account to do the fourier transformation. There are two iTMDs accompanied to twist three LCDAs, corresponding to the two-particle and three-particle terms, respectively. Two transversal-size parameters are hence involved, in which  $\beta'^2$  is expected to be smaller than  $\beta^2$  since the color charged soft gluon would shrink up the transversal extent of hadrons.

## 2.2 Electromagnetic form factor of pion

The electromagnetic form factor of pion meson has been investigated in the QCD and factorization theorem for several decades. From the theoretical side, the QCD-based calculations are almost carried out for the spacelike form factors, and different approaches have their own favorite momentum transfers. For example, the Dyson-Schwinger equation (DSE) applies in the low momentum transfers [41, 42], the light-cone sum rules (LCSRs) prediction is valid in the low and intermediate momentum transfers [20, 22], and the perturbative QCD (pQCD) is powerful in the process with large momentum transfer [43, 44]. More impressively, the lattice QCD (LQCD) have recently improved their evaluation from the region  $-1 \text{ GeV}^2 \leq q^2 \leq 0$  [45] to  $-10 \text{ GeV}^2 \leq q^2 \leq 0$  [46]. From the experimental side, the precise measurement is only available in the timelike physical region. The result with the invariant mass  $4m_\pi^2 \leq s \lesssim 8.7 \text{ GeV}^2$  is reported by the BABAR collaboration [47], and the isospin-vector form factor in  $4m_\pi^2 \leq s \leq 3.125 \text{ GeV}^2$  is measured via the  $\tau$  decays by the Belle collaboration [48]. The BESIII collaboration also published their result in the  $\rho - \omega$  region [49] based on the initial state radiation (ISR) method. There are also some data on the spacelike form factor measured via the electron-nucleon elastic scattering [50] and the electron produced pion meson process  $^1H(e, e'\pi^+)n$  [51, 52], but they are only available in the small momentum transfers  $-2.50 \text{ GeV}^2 \leq q^2 \leq -0.25 \text{ GeV}^2$ . With the completion of the 12 GeV Upgrade at Jefferson Laboratory, the 12 GeV beam energy corresponds to 9 GeV photons [53], one can expect more excite data in the space-like regions.

People usually take use of the dispersion relation to connect the QCD predictions of the spacelike form factor to the experimental measurement of the timelike one.

$$\mathcal{F}_\pi^{\text{pQCD}}(q^2) = \frac{1}{\pi} \int_{s_0}^{\infty} ds \frac{\text{Im}\mathcal{F}_\pi(s)}{s - q^2 - i\epsilon}, \quad q^2 < s_0. \quad (2.30)$$

In the standard dispersion relation, the integrand is the imaginary part of timelike form factor. Therefore, in a practice one has to firstly parameterize the form factor data in a resonant model, this brings an additional uncertainty inevitably. We propose to use the modular representation of the dispersion relation [22, 44], where the imaginary part is substituted by the absolute value, hence the model dependence is eliminated by forwarding directly the measurement data.

$$\mathcal{F}_\pi^{\text{pQCD}}(q^2) = \exp \left[ \frac{q^2 \sqrt{s_0 - q^2}}{2\pi} \int_{s_0}^{\infty} ds \frac{\ln |\mathcal{F}_\pi(s)|^2}{s \sqrt{s - s_0} (s - q^2)} \right], \quad q^2 < s_0. \quad (2.31)$$

The derivation of modular dispersion relation can be found in appendix C. The modulus square in the integrand is written in terms of heavy theta functions

$$|\mathcal{F}_\pi(s)|^2 = \Theta(s_{\text{max}} - s) |\mathcal{F}_{\pi, \text{Inter.}}^{\text{data}}(s)|^2 + \Theta(s - s_{\text{max}}) |\mathcal{F}_\pi^{\text{pQCD}}(s)|^2, \quad (2.32)$$

in which the available data ( $4m_\pi^2 \leq s \leq s_{\max} \simeq 8.7 \text{ GeV}^2$ ) are interpolated with evenly distribution with the interval  $0.01 \text{ GeV}$ , and the high energy tail is well calculated by the pQCD approach<sup>1</sup>. We mark that the modular dispersion relation shown in Eq. (2.31) strengthens the role of high energy tail in the dispersion relation with the logarithm of the timelike form factor, we will discuss again this in the numerics.

In the pQCD calculation of pion and kaon EMFFs, the terms from twist three LCDAs give the dominate contributions, rather than the leading twist LCDAs. This is different from the LCSRs prediction [20–22] where only the even twist LCDAs survive, hence the EMFFs are predominated by the leading twist LCDAs. The dominate twist three contribution in pQCD does not indicate a destruction of the power expansion, but an effect of the chiral enhancement in the processes involving pseudoscalar mesons. As we see in equations (2.7,2.8), the contributions from the leading twist, two-parton twist-3, twist-2  $\otimes$  twist-4, three-parton twist-3 and twist-4 LCDAs to the EMFFs obey the power behavior

$$\begin{aligned} & \mathcal{F}_P^{t2}(Q^2) : \mathcal{F}_P^{2p,t3}(Q^2) : \mathcal{F}_P^{2p,t2\otimes t4}(Q^2) : \mathcal{F}_P^{3p,t3}(Q^2) : \mathcal{F}_P^{3p,t4}(Q^2) \\ &= \mathcal{O}(1) : \mathcal{O}\left(\frac{m_0^2}{\tilde{Q}^2}\right) : \mathcal{O}\left(\frac{\delta_P^2}{\tilde{Q}^2}\right) : \mathcal{O}\left(\frac{f_{3P}^2}{f_P^2 \tilde{Q}^2}\right) : \mathcal{O}\left(\frac{\delta_P^4}{\tilde{Q}^4}\right). \end{aligned} \quad (2.33)$$

Here  $f_P, f_{3P}$  are decay constants defined in equation (2.9),  $\delta_P$  is the parameter in the two-particle twist four LCDAs, and the chiral mass is defined by  $m_0^P \equiv \frac{m_P^2}{(m_{q_1} + m_{q_2})}$ . We have clarified that the  $k_T$  and threshold resummations result to the sudakov functions which suppress in sharp the contributions from the small  $k_T$  and end-points, and pick out the contributions at small  $x \sim \mathcal{O}(0.1)$  and  $k_T \sim \mathcal{O}(0.1Q^2)$  in the multiple integration. The effective longitudinal virtuality  $\tilde{Q}^2$  in the hard scattering grows much slowly than the momentum transfers  $Q^2$ , hence the chiral enhancement emerges in the intermediate and large momentum transfers<sup>2</sup>. Besides the chiral enhancement of the two-particle twist three LCDAs, the contributions from other LCDAs are checked to satisfy the rigorous hierarchy of power expansion [22].

We immediately conclude that the chiral mass  $m_0^\pi$  and the lowest order gegenbauer coefficient  $a_2^\pi$  are the most two important parameters in the pQCD calculation of pion EMFF. Inspired by this, we rewrite the pQCD expression in equations (2.7,2.8) in terms of these two parameters

$$\begin{aligned} \mathcal{F}_\pi^{\text{em}}(Q^2) &= (m_0^\pi)^2 \mathcal{F}_{\pi,1}^{\text{em}}(Q^2) + m_0^\pi m_\pi \mathcal{F}_{\pi,2}^{\text{em}}(Q^2) + m_0^\pi m_\pi a_2^\pi \mathcal{F}_{\pi,3}^{\text{em}}(Q^2) \\ &+ a_2^\pi \mathcal{F}_{\pi,4}^{\text{pQCD}}(Q^2) + (a_2^\pi)^2 \mathcal{F}_{\pi,5}^{\text{em}}(Q^2) + \mathcal{F}_{\pi,6}^{\text{em}}(Q^2). \end{aligned} \quad (2.34)$$

The first row shows the contributions with twist three LCDAs  $\phi^{p,\sigma}$  both in the initial and final states, in which the first term gives the purely asymptotic terms, the second and third

<sup>1</sup>Timelike form factor described by the resonant models [47] deviates from the asymptotic behavior  $\mathcal{F}_\pi(q^2) \sim 1/q^2$  at large momentum transfers, this is the other reason to take pQCD calculation to describe the high energy tails.

<sup>2</sup>The leading twist contribution begins to be dominate at an ultraviolet scale like  $m_Z^2$  [54].

**Table 1.** Input parameters of pion meson in the pQCD calculations.

$f_{3\pi}(10^{-2})$ [8]	$a_2^\pi$ [22]	$a_4^\pi$ [22]	$\omega_{3\pi}$ [8]	$\delta_\pi^2$ [8]	$\omega_{4\pi}$ [8]
$0.45 \pm 0.15$	$0.28 \pm 0.05$	$0.19 \pm 0.06$	$-1.50 \pm 0.70$	$0.18 \pm 0.06$	$0.20 \pm 0.10$

terms indicate the convolution of asymptotic term and quark mass suppressed term. The first two terms in the second row show the contributions from the lowest gegenbeur polynomials in the leading twist LCDAs, and the last term  $\mathcal{F}_{\pi,6}^{\text{em}}$  is the summation of asymptotic contribution from leading twist LCDAs and the retaining higher twist LCDAs, like two-particle twist four and three-particle LCDAs.  $\mathcal{F}_{\pi,i}^{\text{em}}$  are invariant functions which are not dependent on  $m_0$  and  $a_2^\pi$ .

Substituting the pQCD expression in equation (2.34) into the dispersion relation in equation (2.32), we can extract out the  $m_0^\pi$  and  $a_2^\pi$  with the input data in the physical regions. While, in practice, we are only able to obtain a reliable result for  $m_0^\pi$ , the fit result of  $a_2^\pi$  is out of control with a large uncertainty which is traced to the non-leading role of leading twist contribution. Since the LQCD evaluations only hold well for the lowest gegenbauer coefficient  $a_2$  so far, we take the result obtained from the joint analysis of electromagnetic form factor with modular dispersion relation and precise LCSRs calculation [22], they are shown in table 1 as well as other parameters of pion LCDAs. We take  $m_\pi = 0.14$  GeV and  $f_\pi = 0.13$  GeV,  $f_{3\pi}$  and  $\delta_\pi^2$  are in unit of  $\text{GeV}^2$ .

We consider two versions of pQCD calculations in the form factor fitting. One is the sudakov function-predominated picture [40] in which only the hard transversal degree of freedom is pick out in the sudakov exponential. The other one is the sudakov plus gaussian picture in which the soft transversal degree of freedom are also considered in the iTMDs [37]. In the sudakov plus gaussian picture, the transversal-size parameter accompanied to valence state is chosen at  $\beta_\pi^2 = 0.511_{-0.035}^{+0.040}$  based on Eq. (2.23). Three-particle state also contribute to the two-particle (power) twist three LCDAs with the equation of motion. As we see from the  $\rho_\pm^{\mathcal{P}}$  terms shown in Eqs. (B.2,B.3), this part is proportional to the quark masses, hence it can be safely neglected in the pion case. In the pQCD calculation of pion form factor we would not consider the iTMD function  $\Sigma'$  in Eq. (2.29).

Table 2 show the fit result of chiral mass. Scenarios A (B) denotes the fit with (without) considering the scale evolution of nonperturbative parameters appeared in the LCDAs. The result shown in Set-I is obtained under the sudakov factor-predominated picture in the deep virtual Euclidean momenta space  $-30 \leq q^2 \leq -10 \text{ GeV}^2$ . The results in Set-II indicates the fit in the momentum transfers  $-30 \leq q^2 \leq -5 \text{ GeV}^2$  under the sudakov

**Table 2.**  $m_0^\pi$  obtained by matching the pQCD calculations to the modular dispersion relation.

Set	IA	IB	IIA	IIB
$m_0^\pi(\text{GeV})$	$1.37 \pm 0.10$	$1.30 \pm 0.10$	$1.54 \pm 0.06$	$1.84 \pm 0.07$

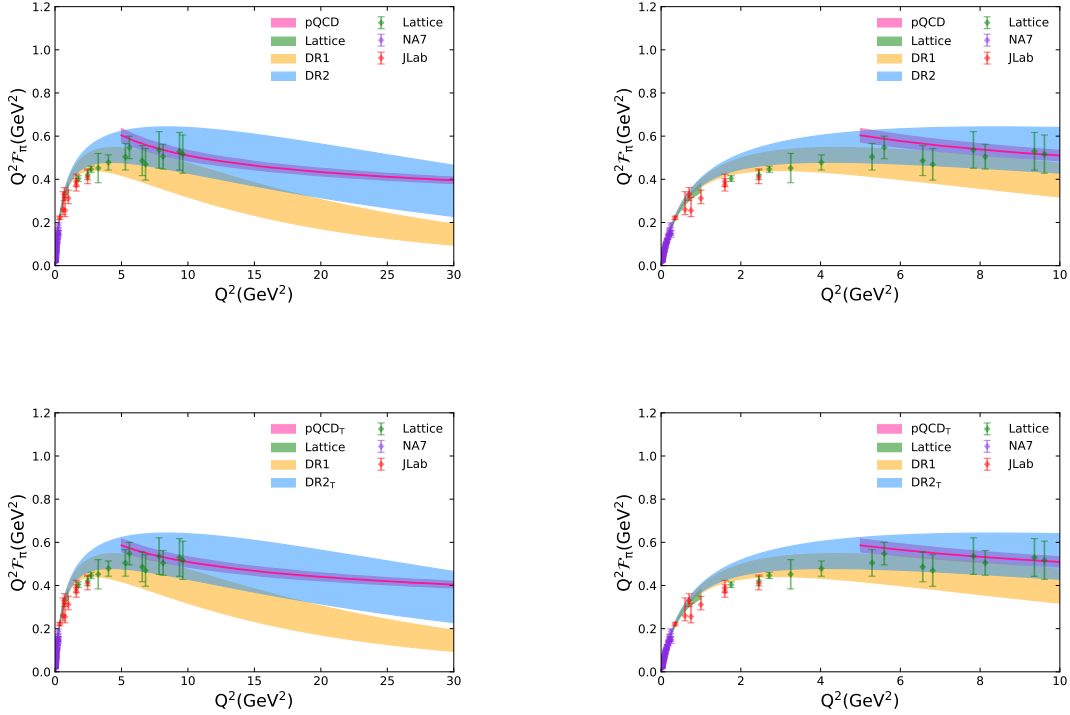


**Figure 2.** Up:  $Q^2 \mathcal{F}_\pi(Q^2)$  obtained under the sudakov factor-predominated picture in  $5 \leq Q^2 \leq 30$   $\text{GeV}^2$ . Low: Result obtained under the sudakov plus gaussian picture in  $5 \leq Q^2 \leq 30$   $\text{GeV}^2$ .

plus gaussian picture. We notice that the pQCD prediction of the timelike form factor is embodied in the dispersion integral as the high energy tail contribution in equation (2.31), in which the  $m_0^\pi$  terms can not be separated out in the logarithm. So in the fit we firstly take an initial value of chiral mass ( $1.6 \pm 0.4$   $\text{GeV}$ ) for the high energy tail contribution in the integrand, and do the numerical iteration to find the optional value of  $m_0^\pi$  with the modular dispersion relation.

With the chiral mass obtained in table 2, we plot in figure 2 the spacelike form factor  $Q^2 \mathcal{F}_\pi(Q^2)$ . The up (down) row shows the result obtained in scenario IB (IIB) where the result obtained from the modular dispersion relation is compared to the pQCD prediction. In the right panel, we show the enlargement in the momentum transfers  $0 \leq Q^2 \leq 10$   $\text{GeV}^2$ . The blue (DR2) and yellow (DR1) bands show dispersion relation result with and without including the high energy tail in the dispersion integrand, respectively. We also depict the available measurements from NA7 [50] and Jefferson Lab [51, 52], and the recent lattice QCD evaluations [45, 46]. In figure 3, we depict the pion EMFF in the whole kinematics, in which the iTMDs-improved pQCD predictions are shown in magenta bands.

We give some intermediate conclusions.

- (a) In the modular dispersion relation (2.31), the contribution from high energy tail is not highly suppressed as expected from the standard dispersion relation (2.30). This is seen from the gap between the blue (DR2) and yellow bands (DR1), and can be

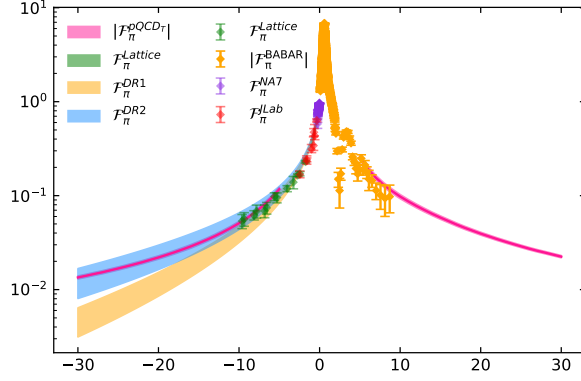


**Figure 3.** EMFFs of pion meson in the whole kinematical region.

traced back to logarithm expression and the subtraction factor  $q^2 \sqrt{s_0 - q^2}$  in the numerator.

- (b) The spacelike form factor obtained from the modular dispersion relation does not sensitive to iTMD function. This is not surprise because the iTMD function only modify the form factor in the small momentum transfer regions, while in the modular dispersion relation the pQCD calculation is called in the large momentum transfers.
- (c) For the direct pQCD calculation of spacelike form factor shown in the left hand side of equation (2.31), the iTMD functions indeed suppress the result in the small and intermediate momentum transfer regions and hence improve the prediction power to a few  $\text{GeV}^2$ . The effect from iTMDs is tiny in the large momentum transfers. From the other hand, as claimed in (b), the spacelike result obtained from dispersion relation does not sensitive to iTMD function. That's why the chiral mass obtained from the sudakov plus gaussian picture (Set-II) is much larger than that obtained from the sudakov factor-predominated picture (Set-I).
- (d) The chiral mass obtained by fitting the iTMDs-improved pQCD prediction to dispersion relation is  $m_0^\pi(1\text{GeV}) = 1.84 \pm 0.07$ . This value is thirty percents larger than the previous pQCD result  $1.30 \pm 0.10$ , but consists with the ChPT [71], indicating a sizable decrease of form factor due to the soft transversal dynamics, especially in the small and intermediate momentum transfers.

### 2.3 Electromagnetic form factor of kaon

We turn to the EMFFs of kaon meson. Depict its lack of measurement in the spacelike region, there are abundant data of the timelike form factor. Such as the earlier result in the energy region  $1.40 - 2.18 \text{ GeV}$  detected by the magnetic detector DM1 [56, 57] and the result in the region  $1.35 - 2.40 \text{ GeV}$  measured by the DM2 detector at the Orsay storage rings DCI[58]. The result are also obtained in the  $1.0 - 1.4 \text{ GeV}$  from the OLYA

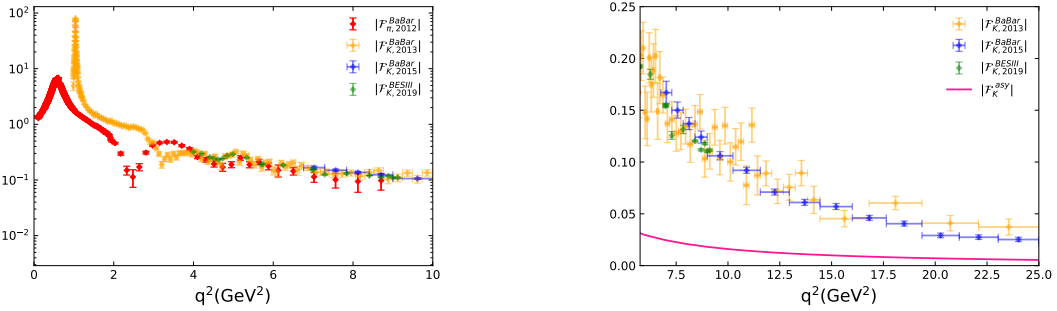


**Figure 4.** Left: Timelike EMFFs of pion and kaon measured from the thresholds to 10 GeV<sup>2</sup>. Right: Kaon EMFF measured in the large momentum transfers.

detector [59, 60], at  $\phi(1020)$  point [61] and in the energy region  $\sqrt{q^2} = 1.04 - 1.38$  GeV [62] from the SND detector, and in the  $\phi(1020)$  region 1.01 – 1.034 GeV from the CMD2 [63] detector at VEPP-2M Collider. The result at a high energy point  $q^2 = 13.48$  GeV<sup>2</sup> is then obtained with the CLEO-c detector [64, 65]. What’s more, the result from the threshold to 5 GeV [66] and from 2.6 to 8.0 GeV [67] are measured from the BaBar collaboration at PEP-II2  $e^+e^-$  collider with the ISR method. Recently, the BESIII detector at BEPCII reported the most precise measurement of the result in the energy region  $\sqrt{q^2} = 2.00 - 3.08$  GeV [68].

We depict the recent measurements of kaon EMFFs from the BaBar and the BESIII collaborations in figure 4. For the sake of comparison to the available BaBar measurement of pion EMFFs, the data is truncated up to the energy 10 GeV<sup>2</sup>. The measurement of pion form factor [47] was fitted to a superposition of four  $\rho$  resonances, starting from  $\rho(770)$ , including the three subsequent radial excitations  $\rho(1450)$ ,  $\rho''(1700)$ ,  $\rho'''(2250)$  and taking into account the  $\rho - \omega$  mixing. In this model, the  $\rho$  resonances and the  $\omega$  resonance are described by the Gounaris-Sakurai (GS) [69] and the Kühn-Santamaria (KS) representation [70] of the Breit-Wigner function, respectively. For the kaon form factor [66], the similar Breit-Wigner functions are used for totally eleven resonances to fit the data in the energy region  $4m_K^2 \leq q^2 \leq 2.4^2$  GeV<sup>2</sup>, including three  $\phi$  (1020, 1680, 2170), four  $\rho$  (770, 1450, 1700, 2250) and four  $\omega$  (782, 1420, 1650, 2200). At higher energy region  $2.4^2 \leq q^2 \leq 5^2$  GeV<sup>2</sup> where the perturbative calculation is reliable, the squared form factor is fitted by the function  $A\alpha_s(q^2)/s^n$ . The fit parameter  $n = 2.04 \pm 0.22$  [47, 66] agrees with the QCD asymptotic behavior [3, 4]  $\mathcal{F}_K^{\text{asy}}(q^2) = 8\pi\alpha_s(q^2)f_K^2/q^2$ , while it shows about four times larger in magnitude when we take the decay constant  $f_K = 0.156$  GeV from the lattice evaluation [39]. This derivation, as we can see in the right panel of figure 4, reveals the significant non-asymptotic contributions which mainly arises from the chiral enhancement effect of the two-particle twist three LCDAs.

In the figure 5, we compare the kaon and pion EMFFs measured by BaBar collaboration. We depict the available data (left) and their ratios (right) in the energy region  $5 \leq q^2 \leq 8.7$  GeV<sup>2</sup>. The choice of this region is twofold considerations. Firstly, the BaBar



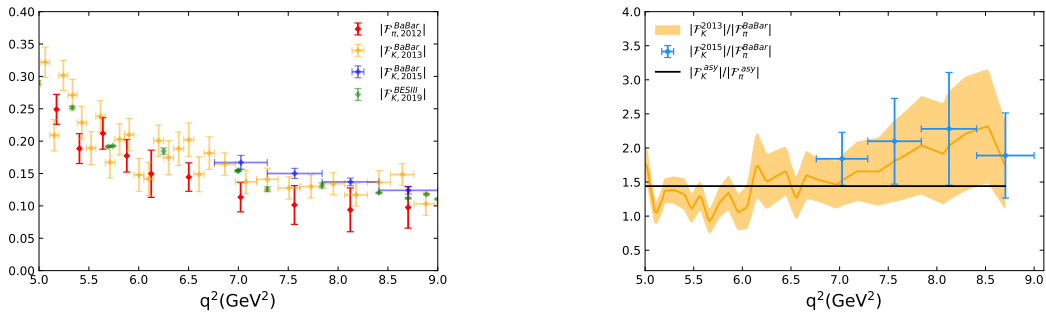


**Figure 5.** Left: Kaon and pion EMFFs measured in the energy region  $5 \leq q^2 \leq 8.7 \text{ GeV}^2$ . Right: The ratios of Kaon and pion EMFFs data.

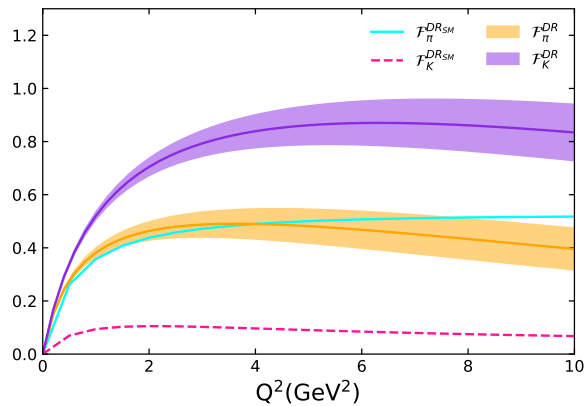


**Figure 6.** EMFFs obtained from the standard (curves) and modular (bands) dispersion relations.

data of pion form factor is available up to  $8.7 \text{ GeV}^2$ . And secondly this region is already away from the physical region, hence it is clear without resonances background. We notice that the 2013 data of kaon form factor is measured at different energy points within also different bins, in contrast to the pion form factor. So we depict the ratio  $|\mathcal{F}_{K,2013}^{\text{BaBar}}|/|\mathcal{F}_{\pi,2012}^{\text{BaBar}}|$  (yellow data points) by interpolating their data in the available energy regions. For the data measured in 2015, the energy points and bins are chosen as the same as the measurement of pion form factor, we then show the ratio  $|\mathcal{F}_{K,2015}^{\text{BaBar}}|/|\mathcal{F}_{\pi,2012}^{\text{BaBar}}|$  directly at four energy points (blue data points). The squared errors mainly comes from the pion form factor. We also depict the asymptotic pQCD predictions (black line)  $|F_K^{\text{asy}}(q^2)|/|F_\pi^{\text{asy}}(q^2)| = f_K^2/f_\pi^2 = 1.44$  for the comparison. The ratio is found to be close to the asymptotic value in the intermediate momentum transfers. While in the large transfers  $7 \leq q^2 \leq 9 \text{ GeV}^2$ , the central values of ratios begin to deviate from the asymptotic value, especially when we consider the measurement in 2015 [67]. This deviation reveals a sizable  $SU(3)$  breaking in the LCDAs of pion and mesons, besides their decay constants.

With the precise measurement of kaon EMFFs in timelike regions, we can obtain the spacelike form factors with the dispersion relations. In figure 6 we show the result of

kaon form factors obtained from the standard (magenta curve) and modular (purple band) dispersion relations without considering the high energy tails contributions. For the sake of comparison, we also depict the result of pion form factors in cyan curve and yellow band. We found the result of pion EMFF obtained from the standard dispersion relation is very close to that obtained from the modular one. This consistence, from one side, convinces us that the GS and KS resonant models [47] pick up the right imaginary part. And from the another side, it checks the assumption that  $\mathcal{F}_\pi(q^2)$  has no zero value in the complex plane in the derivation of modular dispersion relation [22, 44].

For the kaon form factor, however, the modular dispersion relation gives much larger result in contrast to the standard dispersion relation. The modular dispersion relation deduced result is comparable to the pion form factor, if we consider a reasonable large  $SU(3)$  breaking effect. So firstly, we think that the resonant model adopted by BaBar collaboration [66] does not capture the right imaginary part of timelike kaon form factor, even though it describes the absolute value well. And secondly, the modular dispersion relation might not holds well for the kaon form factor. In principle, the charged form factor extracted at BaBar detector via  $e^+e^-$  annihilation includes both the contributions from  $P$ -wave and  $S$ -wave resonances, even if the later one is suppressed by the phase space. The isospin scalar  $S$ -wave contribution to the form factor might have a sharp dip around  $f_0$ , hence destroys the modular dispersion relation. So that we do not take the dispersion relations in the study of kaon EMFFs, but fit the pQCD calculation directly to the measurement in the broad timelike regions  $10 \leq q^2 \leq 60 \text{ GeV}^2$ .

In terms of chiral mass, the pQCD result in equations (2.7,2.8) is modified to

$$\begin{aligned} \mathcal{F}_K^{\text{em}}(q^2) &= (m_0^K)^2 \mathcal{F}_{K,1}^{\text{em}}(q^2) + m_0^K m_K \mathcal{F}_{K,2}^{\text{em}}(q^2) \\ &+ m_0^K m_K a_1^K \mathcal{F}_{K,3}^{\text{em}}(q^2) + \mathcal{F}_{K,4}^{\text{em}}(q^2). \end{aligned} \quad (2.35)$$

Here the first term comes from the two-particle twist three LCDAs, the second and third terms mainly come from the interplay between the leading twist LCDAs (in particular, the asymptotic term and the first gegenbauer expansion term) and the two-particle twist three LCDAs, the last term collects the remaining contributions from higher gegenbauer terms in leading twist LCDAs and from the high twist LCDAs. The well-known chiral perturbative theory (ChPT) relations [71]

$$\begin{aligned} \mathcal{R} &\equiv \frac{2m_s}{m_u + m_d} = 24.4 \pm 1.5, \\ \mathcal{Q}^2 &\equiv \frac{m_s^2 - (m_u + m_d)^2/4}{m_d^2 - m_u^2} = (22.7 \pm 0.8)^2 \end{aligned} \quad (2.36)$$

results in the chiral mass without involving the light quark masses  $m_u$  and  $m_d$ .

$$m_0^K(1\text{GeV}) = \frac{m_K^2}{m_s \left[1 + \frac{1}{\mathcal{R}} \left(1 - \frac{\mathcal{R}^2 - 1}{4\mathcal{Q}^2}\right)\right]} = 1.90 \text{ GeV}. \quad (2.37)$$

**Table 3.** Input parameters of kaon meson in the pQCD calculations.

$m_K$ [39]	$m_0^K$ [71]	$f_K$ [39]		$a_1^K$ [55]	$a_2^K$ [55]
0.50	1.90	0.16		$0.05 \pm 0.00$	$0.11 \pm 0.02$
$f_{3K}(10^{-2})$ [8]	$\omega_{3K}$ [8]	$\lambda_{3K}$ [8]	$\delta_K^2$ [8]	$\omega_{4K}$ [8]	$\kappa_{4K}$ [8]
$0.45 \pm 0.15$	$-1.2 \pm 0.7$	$1.6 \pm 0.4$	$0.20 \pm 0.06$	$0.20 \pm 0.10$	$-0.12 \pm 0.01$

We take the current quark mass  $\overline{m}_s(2 \text{ GeV}) = 96_{-4}^{+8} \text{ MeV}$  [39]. As we have claimed above that the chiral enhancement effect makes it is powerless to fit  $a_n^K$  via the EMFFs, so we taken them as the input as well as other parameters which are collected in table 3.

With the twist three LCDAs  $\phi^{s,\sigma}(u, \mathbf{k}_T)$  formulized in equation (2.24) and the associated soft iTMD functions expressed in equation (2.26) and equations (2.20,2.29), we separate the contribution from the valence quark state and  $q\bar{q}g$  state. The invariant functions  $\mathcal{F}_{K,1}^{\text{em}}$  and  $\mathcal{F}_{K,2}^{\text{em}}$  in equation (2.35) are rewritten in terms of the dimensionless parameter  $\rho_K = m_s/m_0^K$ .

$$\begin{aligned}\mathcal{F}_{K,1}^{\text{em}}(q^2) &= \mathcal{F}_{K,1}^{\text{a}}(q^2) + \rho_K \mathcal{F}_{K,1}^{\text{b}}(q^2) + \rho_K^2 \mathcal{F}_{K,1}^{\text{c}}(q^2), \\ \mathcal{F}_{K,2}^{\text{em}}(q^2) &= \mathcal{F}_{K,2}^{\text{a}}(q^2) + \rho_K \mathcal{F}_{K,2}^{\text{b}}(q^2).\end{aligned}\quad (2.38)$$

Here  $\mathcal{F}_{K,1}^{\text{a}}$  and  $\mathcal{F}_{K,1}^{\text{c}}$  in the first row denote the contribution from purely valence quark state  $\phi_{K,2p}^{p,\sigma}$  and purely  $q\bar{q}g$  states  $\phi_{K,3p}^{p,\sigma}$ , respectively, meanwhile,  $\mathcal{F}_{K,1}^{\text{b}}(q^2)$  stands for the interplay contribution between them. In the second row,  $\mathcal{F}_{K,2}^{\text{a}}$  is proportional to the leading twist LCDAs  $\phi_K$  and the twist three LCDAs  $\phi_{2p}^{p,\sigma}$  from valence quark state.

We are now able to extract the transversal-size parameter  $\beta_K^2$  by fitting the pQCD calculations to the precise BaBar measurement in the large momentum transfers  $q^2 \geq 7.0 \text{ GeV}^2$ . The extracted result  $\beta_K^2 = 0.30 \pm 0.05 \text{ GeV}^{-2}$  indicates the mean transversal momentum  $[\langle \mathbf{k}_T^2 \rangle]^{1/2} = 0.55 \pm 0.07 \text{ MeV}$  for valence quark state at leading twist. The three-particle contribution in twist three LCDAs  $\phi_{2p}^{p,\sigma}$  is proportional to  $\mathcal{O}(m_s/m_0^K)$ , the current accuracy from both the measurement and pQCD calculation can not help us to extract the value of transversal-size parameters associated to  $\bar{q}qg$  state. In the numerics, we take it no larger than the transversal-size parameter of  $\pi$  meson  $\beta_K'^2 < 0.511 \text{ GeV}^{-2}$ . In table 4, we list the mean transversal momentum defined in equation (2.22), and the conjugated distances of  $\pi, K$  mesons associated to two-particle LCDAs at different twists. The mean transversal momenta of pion and kaon mesons are at soft scale, the conjugated distances are smaller than their charge radius<sup>3</sup>, respectively. The slight difference of the mean values between leading twist and twist three LCDAs comes from the three-particle iTMD contribution.

With the fit result of the iTMD functions, we plot in figure 7 the pQCD predictions of kaon EMFFs in the large momentum transfers  $|q^2| \leq 10 \text{ GeV}^2$ . The result obtained with

<sup>3</sup>The mean square electric charge radius of the kaon is  $\langle r_K^2 \rangle^{1/2} = 0.56 \pm 0.03 \text{ fm}$ , this value is smaller than the charge radius of pion  $\langle r_\pi^2 \rangle^{1/2} = 0.67 \pm 0.08 \text{ fm}$  [39].

**Table 4.** The mean transversal momenta and the conjugated distances of  $\pi, K$  mesons associated to leading twist and twist three LCDAs.

mean value	$\phi$	$\phi^p$	$\phi^\sigma$
$\langle k_T^2 \rangle_\pi^{1/2}$ (GeV)	$0.36 \pm 0.02$	$0.40 \pm 0.02$	$0.40 \pm 0.02$
$\langle b_T^2 \rangle_\pi^{1/2}$ (fm)	$0.56 \pm 0.02$	$0.50 \pm 0.02$	$0.50 \pm 0.02$
$\langle k_T^2 \rangle_K^{1/2}$ (GeV)	$0.55 \pm 0.07$	$0.53 \pm 0.07$	$0.52 \pm 0.07$
$\langle b_T^2 \rangle_K^{1/2}$ (fm)	$0.37 \pm 0.05$	$0.38 \pm 0.05$	$0.39 \pm 0.05$

(without) considering the iTMDs are shown in magenta and yellow bands, respectively. In comparison, the BaBar measurements [66, 67] and the recent lattice result [46, 72] are superposed. We see that iTMDs are indispensable to explain the timelike data  $|\mathcal{F}_K(q^2)|$  in the intermediate and large  $q^2$ . The iTMDs-improved pQCD prediction (magenta band)  $Q^2 \mathcal{F}_K(q^2)$  shows a small result in comparing to the lattice evaluation [46]. This difference is understood by the significant  $SU(3)$  flavor breaking of kaon meson, which emerges additional terms, proportional to  $s$ -quark mass, in the twist three LCDAs of kaon meson. We can see from the pQCD result with taking  $m_s = 0$  terms (yellow band) that these terms decrease the pQCD prediction by 30% to 35%. We mark that the lattice result still have large uncertainty in the large  $q^2$  region, and our result agrees with the DSE approaches [73] and the collinear QCD factorization [74]. The inclusion of iTMDs also improves the power of pQCD prediction down to a few  $\text{GeV}^2$  as we have already seen in the pion case.

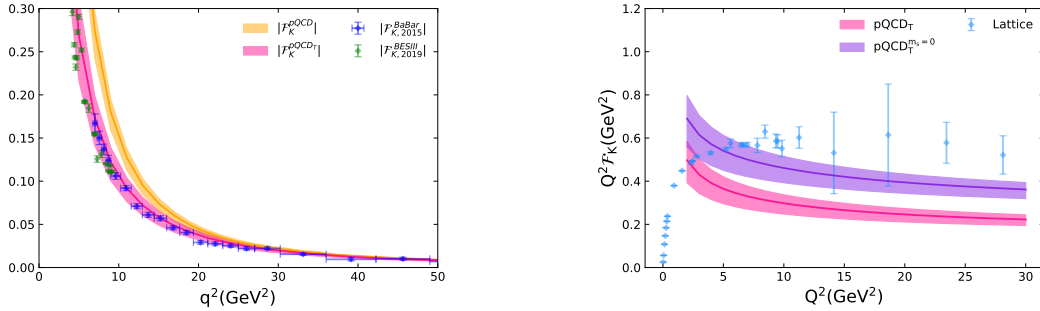


**Figure 7.** The pQCD predictions of timelike (left) and spacelike (right) kaon EMFFs.

### 3 Meson-Photon transition form factors

The meson-photon TFFs provide another excellent playground to study light-cone distribution amplitudes. Due to the conservation of chiral-symmetry of electromagnetic currents  $j_\mu^{\text{em}} = e_u \bar{u} \gamma_\mu u + e_d \bar{d} \gamma_\mu d + e_s \bar{s} \gamma_\mu s$ , the chiral-odd LCDAs defined in equations (A.2, A.3) do not give contribution to the TFFs, only the LCDAs defined by the chiral-even quark operator  $\bar{q}(z_2) \gamma_\rho \gamma_5 q(z_1)$  in equation (A.1) contribute to the TFFs. In this sense, theoretical

speaking, it is hence clean to investigate the shape of leading twist LCDAs in the TFFs of pseudoscalar mesons [44].

40 years ago, Lepage and Brodsky proposed the perturbative QCD to explain the TFFs measurements [4]. The first systematical measurement is done by the CELLO detector [75] in the photonic production of a single pseudoscalar meson  $e^+e^- \rightarrow e^+e^- [\gamma\gamma^* \rightarrow] \mathcal{P}$ , here  $\mathcal{P} = \pi^0, \eta, \eta'$ . At the small momentum transfers, saying  $Q^2 < 2.7 \text{ GeV}^2$  and  $Q^2 < 3.4 \text{ GeV}^2$  for the  $\pi^0$  and  $\eta^{(\prime)}$  TFFs respectively, the CELLO data could be explained well in the vector meson dominance model (VMD) with a simple  $\rho$ -pole [76], and also in the QCD inspired Brodsky-Lepage model [77]. More important, the neutral pion TFF is well in accord with the charged one, it resolves the long standing confusion about the slope sign of the neutral form factor. These form factors are later measured at larger momentum transfers ( $1.9 \leq Q^2 \leq 9 \text{ GeV}^2$  for  $\pi^0$  and  $1.5 \leq Q^2 \leq 20(30) \text{ GeV}^2$  for  $\eta(\eta')$ ) by the CLEO-II collaboration [78].

The perturbative QCD prediction of TFFs is expressed as a convolution of hard scattering kernel and the LCDAs of mesons, and the QCD asymptotic behavior reads [77]

$$\lim_{Q^2 \rightarrow \infty} Q^2 \mathcal{F}_{\mathcal{P}\gamma\gamma^*}(Q^2) = \sqrt{2} f_{\mathcal{P}}. \quad (3.1)$$

In parallel, the chiral limit of QCD shows the axial anomaly [79, 80]

$$\lim_{Q^2 \rightarrow 0} \mathcal{F}_{\mathcal{P}\gamma\gamma^*}(Q^2) = \frac{1}{4\pi^2 f_{\mathcal{P}}}. \quad (3.2)$$

The CZ wave functions is proposed [81] to quantify the long-distance nonperturbative effects in a hard exclusive process. However, Kroll concluded that the CZ function of pseudoscalar mesons disagrees with the CLEO-II data. On the contrary, a similar pQCD analysis calculated by Cao, Huang and Ma [82] yielded that neither the asymptotic nor the CZ functions can be excluded by the CLEO-II data. Kroll, Raulfs and Feldman then introduced the iTMD functions, supplementing to the sudakov suppression mechanism, in the pQCD calculation of light pseudoscalar TFFs [83, 84]. This improved the pQCD prediction down to an intermediate transfer momentum, saying a few  $\text{GeV}^2$ .

Meanwhile, Mosatov and Radyushkin developed a sum rules approach to calculate the pion TFF [85] in the region of small momentum transfers. This work is a merging of two different approaches without showing the theoretical uncertainty, hence it is hardly to discriminate the asymptotic and CZ wave functions even though they shown a sufficiently separated curves for the  $\pi^0$  TFF. The TFF is then calculated within an unified framework based on LCSRs [86], in which the long-distance part of the transition is defined by the LCDAs. The leading order result products a correct asymptotic behavior. The LCSRs prediction is powerful in the intermediate and large momentum transfers  $Q^2 \geq 1 \text{ GeV}^2$ , which is much powerful in contrast to QCD sum rules with series vacuum condensates [85]. The radiative corrections and higher twist effects are then considered [87–89] to extract the gegenbauer expansion coefficients in the leading twist pion distribution amplitude. With

the CLEO-II measurement, the precise LCSRs result excluded the asymptotic and the CZ pion distribution amplitudes, indicating a fruitful structure of pion meson.

In 2009, the BaBar collaboration reported their measurement of  $\pi^0, \eta, \eta'$  TFFs with the momentum transfers up to  $40 \text{ GeV}^2$  [90]. The story achieves to the climax because in the large momentum transfer regions  $Q^2 \geq 10 \text{ GeV}^2$ , their result of  $\pi^0$  TFF exceeds the asymptotic QCD limit. These new data created considerable exciting in the theory community. The increase measurement in the large momentum transfers  $Q^2 \geq 10 \text{ GeV}^2$  is understood by convoluting a  $k_T$  dependent hard kernel with a flat DAs [91, 92] in the pQCD calculation [93, 94]. From the view of LCSRs, nevertheless, the unexpected data in the large  $Q^2$  is understood by including more polynomials in the conformal expansion of the leading twist pion DA and taking into account higher twist corrections up to twist-six [95], event though the fit result shows a bad convergence such as  $a_4^\pi > a_2^\pi$ .

The attractive pion TFF is heat off with the measurement from Belle collaboration [96]. The result in the small and intermediate momentum transfers  $Q^2 \leq 9 \text{ GeV}^2$  is agree with other measurements from CELLO, CELO and BaBar collaborations [75, 78, 90]. However, the lineshape in the large  $Q^2 \geq 9 \text{ GeV}^2$  does not display a rapid growth as the BaBar result [90] but shows a consistent with the asymptotic QCD limit. The Belle data then modified the fit result of gegenbauer coefficients  $a_n^\pi$  from the LCSRs calculation [97]. The overall discrepancy between the Belle and BaBar data sets is within 1.5-2 standard deviations. An independent measurement from a third-party is highly expected. The BESIII collaboration has released their result on the pion TFF [98], which showed a good agreement with the CELLO and CLEO results in the small  $Q^2$ . We hope the measurements from Belle-II detector and the future collider experiments would settle down the controversy between the BaBar and Belle data at large  $Q^2$ . Recently, the NNLO correction from the collinear factorization [18] indicates that the two-loop perturbative correction is numerically important to pion TFF. The envisaged precision at Belle-II, with no doubt, would help us to understand the leading twist pion LCDAs much better.

For the TFFs of isospin-zero mesons ( $\eta$  and  $\eta'$ ), the most precise measurements also come from the CLEO [78] and BaBar [99, 100] collaborations. Their results of  $\eta'$  meson show a good consistent, even though the uncertainty is large in the large momentum transfers. While for the  $\eta$  TFFs, their result do not agree well with each other, the BaBar data is  $3\sigma$  lower than the CLEO one at two energy points 7 and 13  $\text{GeV}^2$ . With the BaBar data, one can extract the flavor-basis TFFs  $\mathcal{F}_{\eta_n \gamma \gamma^*}$  and  $\mathcal{F}_{\eta_s \gamma \gamma^*}$  under the simple  $\eta - \eta'$  mixing scheme. In the large  $Q^2$  regions, however, the extracted form factor  $\mathcal{F}_{\eta_n \gamma \gamma^*}$  does not show the rapid increase observed in the  $\pi^0$  TFF [90]. Meanwhile, the extracted  $\mathcal{F}_{\eta_s \gamma \gamma^*}$  lies lower than the pQCD asymptotic value  $2/3f_s \sim 0.12 \text{ GeV}$ . People have tried to understand these discrepancies by considering different models of  $\eta_n, \eta_s$  LCDAs [101–103] and also the two-gluon component in the  $\eta'$  meson [104–106]. The BaBar collaboration then studied the process  $e^+e^- \rightarrow e^+e^-\eta'$  in the double-tag mode and measured the TFF  $\mathcal{F}_{\gamma^* \gamma^* \eta'}$  in the momentum transfer regions  $2 \leq Q_1^2, Q_2^2 \leq 60 \text{ GeV}^2$  [107], which provides a comprehensive testing of pQCD calculation [108].

### 3.1 pQCD formulism

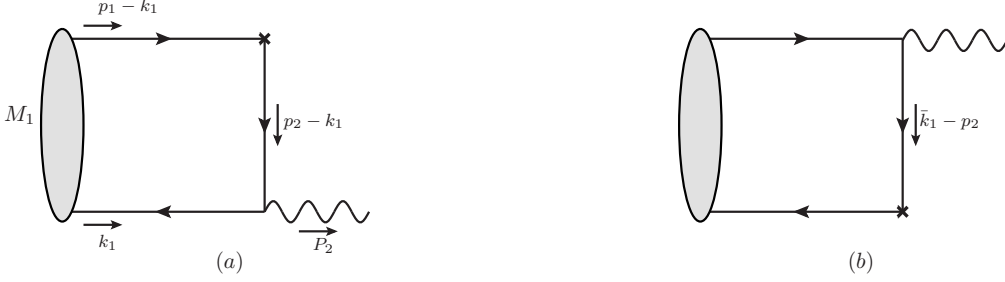


**Figure 8.** Leading-order feynman diagrams of photonic transition process.

In this work, we study the TFFs with including the soft iTMD effects, the operator-production-expansion (OPE) evaluation of LCDAs is improved up to twist four. We focus on the TFFs with one photon virtuality being large and the other photon is on shell. It is defined by the matrix element sandwiched between the neutral meson and the photon state with the electromagnetic current

$$\langle \gamma(p_2, \varepsilon_2^*) | J_\mu^{\text{em}} | \mathcal{P}^0(p_1) \rangle = -i4\pi\alpha\epsilon_{\mu\nu\rho\sigma}\varepsilon_2^{*\nu}p_1^\rho p_2^\sigma \mathcal{F}_{\mathcal{P}\gamma\gamma^*}(Q^2). \quad (3.3)$$

Here  $\alpha$  is the fine structure constant,  $\epsilon_{\mu\nu\rho\sigma}$  is the totally antisymmetric Levi-Civita tensor,  $\varepsilon^\mu$  is the polarization vectors of the virtual photons with the momentum transfer  $Q^2 = -q^2 = -(p_1 - p_2)^2$ , and  $\varepsilon_2^{*\mu}$  is the polarization vector of the real photon with momentum  $p_2$ . In figure 8, we plot the leading-order feynman diagram of meson-photon transitions, where the wave line denotes the emission real photon and the block bullet denotes the electromagnetic vertex. We take the kinematics  $p_1 = (Q/\sqrt{2}, 0, 0)$ ,  $p_2 = (0, Q/\sqrt{2}, 0)$ ,  $k_1 = (xQ/\sqrt{2}, 0, k_T)$  with neglecting the light meson mass.

Similar to the EMFFs of pion meson discussed in the last section, the meson-photon transition matrix element can also be written in the factorization formulization

$$\langle \gamma(p_2) | J_\mu^{\text{em}} | \mathcal{P}^0(p_1) \rangle = \varepsilon_2^{*\nu} \oint dz_1 H_{\alpha\delta}(z_1, 0) \langle 0 | \bar{q}_\gamma(z_1)[z_1, 0] q_\delta(0) | \mathcal{P}^0(p_1) \rangle_{\mu\nu}. \quad (3.4)$$

The hard function at leading order reads as

$$H_{\alpha\delta}^{(0)}(z_1, 0) = (-1) [(ie\gamma_\nu) S^{(0)}(z_1, 0) (ie\gamma_\mu)]_{\alpha\delta}, \quad (3.5)$$

in which  $S^{(0)}$  is the free quark propagator. In the pseudoscalar transition, only the chiral-even term  $\bar{q}\gamma_\rho\gamma_5q$  in the fierz identity Eq. (2.5) survives due to the conservation of chiral symmetry. In this sense, TFFs involve only the leading twist LCDA  $\varphi(u)$  and two-particle twist four LCDAs  $g_{1,2}(u)$ , and it has nothing to do with the twist three LCDAs which brings large pollution to extract leading twist LCDAs in the pion EMFFs due to the chiral enhancement. Summing over the charge factor of electromagnetic currents and the locations of real photon emission shown in figure 8, we arrive at the pQCD prediction of TFFs

at born level

$$\begin{aligned}
\mathcal{F}_{\mathcal{P}\gamma\gamma^*}^{2p}(Q^2) &= e_q^2 \int_0^1 du \int bdb e^{-S(u,b,Q,\mu)} S_t(u, Q) f_{\mathcal{P}} \\
&\cdot \left\{ 2\varphi(u) K_0(\kappa_1 b) \left[ 1 - \frac{\alpha_s(\mu)}{4\pi} C_F \left( \ln \frac{\mu^2 b}{2\kappa_1} + \gamma_E + 2 \ln u + 3 - \frac{\pi^2}{3} \right) \right] \right. \\
&- 4g_1(u) \left[ \frac{b}{2\kappa_1} K_1(\kappa_1 b) + \frac{b}{2\kappa_2} K_1(\kappa_2 b) \right] \\
&\left. - 4\tilde{g}_2(u) \left[ \frac{b}{2\kappa_1} K_1(\kappa_1 b) - \frac{b}{2\alpha_2} K_1(\kappa_2 b) \right] \right\}. \tag{3.6}
\end{aligned}$$

In the above equation,  $K_0$  and  $K_1$  are the second kind of modified Bessel functions (Basset function) of order zero and one, respectively. The variables are  $\kappa_1 = \sqrt{u}Q$  and  $\kappa_2 = \sqrt{\bar{u}}Q$ , and the auxiliary twist four LCDA is defined by  $\tilde{g}_2(u) \equiv \int_0^u du' g_2(u)$ .

The NLO hard gluon correction to the leading twist contribution had been calculated in 2009 by Li and Mishima [35]. In order to take into account the soft gluon correction from the three-particle LCDAs as shown in figure 9, we retain the quark propagator with a zero mass up to the  $\bar{q}qg$  term.

$$\begin{aligned}
S(z_1, z_2) &= \frac{\not{z}_1 - \not{z}_2}{2\pi^2 (z_1 - z_2)^2} \\
&- \frac{\int_0^1 dv G^{\mu\nu}(vz_1 + \bar{v}z_2) \left[ (\not{z}_1 - \not{z}_2) \sigma_{\mu\nu} - 4iv(z_1 - z_2)_\mu \gamma_\nu \right]}{16\pi^2 (z_1 - z_2)^2}. \tag{3.7}
\end{aligned}$$

Here the gluon field  $A_\mu$  is expressed in terms of field strength tensor  $G_{\mu\nu}$ , and the Fock-Schwinger gauge  $z \cdot A(z) = 0$  is taken to guarantee the gauge invariance. The soft gluon corrections to the meson-photon transitions are depicted in figure 9, where the bullets show the possible attaching points of soft gluon. We note that the amplitudes of upper two diagrams with the soft gluon attaching to the external quark lines contributes at the power  $\mathcal{O}(k_T/Q)$ , this contribution could be absorbed into the transversal component of two-particle LCDAs. So the three-particle contribution corresponds to the diagrams where the soft gluon is attached to the internal quark propagator, as shown in the lower two diagrams. The pQCD result for figure 9 (c,d) is

$$\begin{aligned}
\mathcal{F}_{\mathcal{P}\gamma\gamma^*}^{3p}(Q^2) &= e_q^2 \int_0^1 du \int bdb e^{-S(u,b,Q,\mu)} S_t(u, Q) \int_0^u d\alpha_1 \int_0^{\bar{u}} d\alpha_2 \frac{2f_{\mathcal{P}} \varphi_{\parallel}(\alpha_i)}{(1 - \alpha_1 - \alpha_2)^2} \\
&\cdot \left[ (u - \alpha_1) \frac{b}{2\kappa_3} K_1(\kappa_3 b) + (u - \alpha_2) \frac{b}{2\kappa_4} K_1(\kappa_4 b) \right]. \tag{3.8}
\end{aligned}$$

Again, only the chiral-even term  $\bar{q}\gamma_\rho\gamma_5 G^{\rho\sigma} q$  survives in the three-particle LCDAs. The hard scales are  $\kappa_3 = \sqrt{(\alpha_1 + v\alpha_3)}Q$ ,  $\kappa_4 = \sqrt{(\alpha_2 + v\alpha_3)}Q$  and  $v = (u - \alpha_1)/(1 - \alpha_1 - \alpha_2)$ . Combing together the contributions from two particle and three particle LCDAs, the pQCD prediction of meson-photon TFFs is written by

$$\mathcal{F}_{\mathcal{P}\gamma\gamma^*}(Q^2) = \mathcal{F}_{\mathcal{P}\gamma\gamma^*}^{2p}(Q^2) + \mathcal{F}_{\mathcal{P}\gamma\gamma^*}^{3p}(Q^2). \tag{3.9}$$



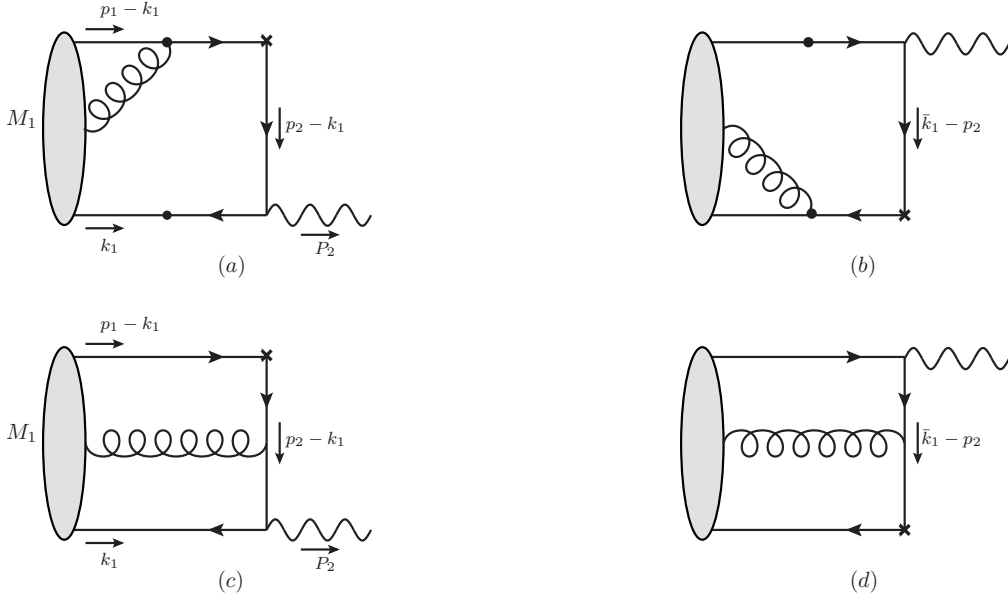


**Figure 9.** The soft gluon corrections to meson-photon TFFs.

### 3.2 Transition form factor of pion

The pion-photon TFF can be decomposed in terms of contributions from different LCDAs.

$$\begin{aligned}
 \mathcal{F}_{\pi\gamma\gamma^*}(Q^2) &= \frac{e_u^2 - e_d^2}{\sqrt{2}} \mathcal{F}_{\mathcal{P}\gamma\gamma^*}(Q^2) \\
 &= \mathcal{F}_{\pi\gamma\gamma^*}^{t2}(Q^2) + \mathcal{F}_{\pi\gamma\gamma^*}^{t4-2p}(Q^2) + \mathcal{F}_{\pi\gamma\gamma^*}^{t4-3p}(Q^2).
 \end{aligned}
 \tag{3.10}$$

Here the contributions from leading twist, two-particle and three-particle twist four LCDAs are written down separately. The prefixal electron charge factor comes from the valence quark distribution in a neutral pion  $|\pi^0\rangle = \frac{1}{\sqrt{2}}|\bar{u}u - \bar{d}d\rangle$ . With the input parameters of pion LCDAs shown in table 1, we depict their contributions in figure 10 (a). The plot shows the expected power hierarchy, in which the leading twist LCDAs give the predominate contribution, and the twist four contributions account only a few percents.

In order to consider the soft transversal dynamics, we supplement the iTMDs to their partner LCDAs in the factorization formulism in Eq. (3.4). For the leading twist contribution, the iTMDs are added directly by Eq. (2.21) with the transversal-size parameter  $\beta_\pi^2 = 0.51 \pm 0.04 \text{ GeV}^{-2}$ . There are two sources to the two-particle twist four LCDAs  $g_{1,2}(u)$ , one is the "genuine" twist four contribution from the three-particle Fock state, the other one is the Wandzura-Wilczek-type mass corrections from the leading twist DAs of the valence quark state, the details is explained in appendix B. The mass corrections terms are proportional to  $m_\pi^2$ , so we can safely drop them in the numerics. And the iTMDs are added to the "genuine" twist four LCDAs  $\varphi_{\parallel,\perp}$  by the three-particle Gaussian function

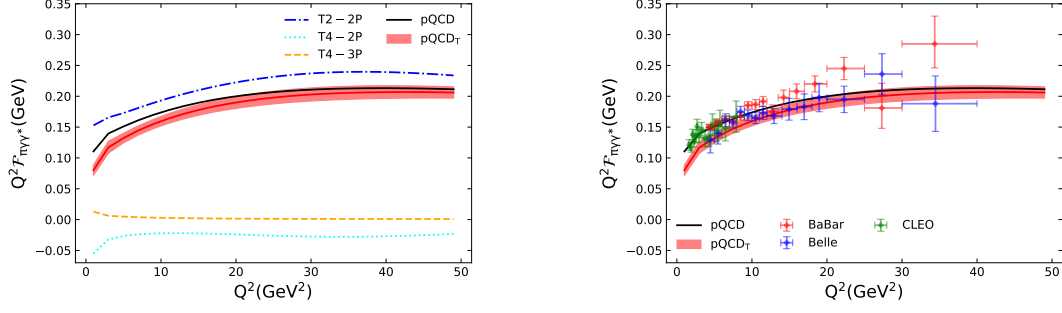


**Figure 10.** Left: Pion-photon TFF  $Q^2 \mathcal{F}_{\pi\gamma^*}$  at different twists, Right: The pQCD prediction of  $Q^2 \mathcal{F}_{\pi\gamma^*}$  in comparison to the measurements.

shown in Eq. (2.29). The pion-photon TFF is then modified to

$$\begin{aligned}
\mathcal{F}_{\pi\gamma^*}(Q^2) = & \frac{e_u^2 - e_d^2}{\sqrt{2}} \int_0^1 du \int bdb e^{-S} S_t f_\pi \left\{ 2\varphi(u) \hat{\Sigma}(u, b) K_0(\kappa_1 b) \right. \\
& \cdot \left[ 1 - \frac{\alpha_s(\mu)}{4\pi} C_F \left( \ln \frac{\mu^2 b}{2\kappa_1} + \gamma_E + 2 \ln u + 3 - \frac{\pi^2}{3} \right) \right] \\
& - 2g_1(u) \left[ \frac{b}{\kappa_1} K_1(\kappa_1 b) + \frac{b}{\kappa_2} K_1(\kappa_2 b) \right] \\
& \left. - 2\tilde{g}_2(u) \left[ \frac{b}{\kappa_1} K_1(\kappa_1 b) - \frac{b}{\kappa_2} K_1(\kappa_2 b) \right] \right\} \\
& + \frac{e_u^2 - e_d^2}{\sqrt{2}} \int_0^1 du \int bdb e^{-S} S_t \int_0^u d\alpha_1 \int_0^{\bar{u}} d\alpha_2 \frac{f_\pi \varphi_{\parallel}(\alpha_i)}{(1 - \alpha_1 - \alpha_2)^2} \\
& \cdot \left[ (u - \alpha_1) \frac{b}{\kappa_3} K_1(\kappa_3 b) + (u - \alpha_2) \frac{b}{\kappa_4} K_1(\kappa_4 b) \right]. \quad (3.11)
\end{aligned}$$

We have set  $b_1 = b_2 = b$  in the iTMD function associated to three-particle state, this is due to the same flavor of the valence quark and antiquark in the pion meson. Because the pion-photon TFF is predominated by the leading twist LCDAs, we do not consider the iTMD correction to the three particle contribution in the numerics. In figure 10 (a), we also depict the result from the iTMDs-improved pQCD calculation (red band). In figure 10 (b), we compare the pQCD predictions of pion-photon TFF to the experiment measurements from CLEO, BaBar and Belle collaborations. We find the introduction of iTMDs decrease the pion-photon TFF in the small and intermediate momentum transfers, while the TFF in the large momentum transfers, saying  $Q^2 \geq 20 \text{ GeV}^2$ , does not sensitive the iTMDs.

### 3.3 Transition form factor of $\eta, \eta'$ mesons

With the isospin symmetry, the valence quark states of  $\eta$  and  $\eta'$  mesons are decomposed in terms of  $SU(3)_F$  singlet-octet states

$$\begin{pmatrix} |\eta\rangle \\ |\eta'\rangle \end{pmatrix} = \begin{pmatrix} \psi_\eta^8 & \psi_\eta^1 \\ \psi_{\eta'}^8 & \psi_{\eta'}^1 \end{pmatrix} \begin{pmatrix} |\eta_8\rangle \\ |\eta_1\rangle \end{pmatrix} = \begin{pmatrix} \cos \theta & -\sin \theta \\ \sin \theta & \cos \theta \end{pmatrix} \begin{pmatrix} \frac{1}{\sqrt{6}} |\bar{u}u + \bar{d}d - 2\bar{s}s\rangle \\ \frac{1}{\sqrt{3}} |\bar{u}u + \bar{d}d + \bar{s}s\rangle \end{pmatrix}. \quad (3.12)$$

Here  $\psi_{\eta^{(i)}}$  describe the opportunity amplitude to find  $\eta^{(i)}$  meson in the flavor singlet and octet states. The exact isospin symmetry implies that the amplitudes can be written in a mixing angle  $\theta$ .

Decay constants of physical states  $\eta^{(i)}$  and singlet-octet states  $\eta_{i=q,s}$  are both defined via the local currents  $J_{\mu 5}^{i=8} = (\bar{u}u + \bar{d}d - 2\bar{s}s) / \sqrt{6}$  and  $J_{\mu 5}^{i=1} = (\bar{u}u + \bar{d}d + \bar{s}s) / \sqrt{3}$ ,

$$\langle 0 | J_{\mu 5}^i | \eta^{(i)}(p) \rangle = i f_{\eta^{(i)}}^i p_\mu, \quad \langle 0 | J_{\mu 5}^i | \eta_i(p) \rangle = i f_{\eta_i} p_\mu. \quad (3.13)$$

It can be read from Eqs. (3.12) that these two types decay constants satisfy the relations

$$\begin{pmatrix} f_\eta^8 & f_\eta^1 \\ f_{\eta'}^8 & f_{\eta'}^1 \end{pmatrix} = \begin{pmatrix} \cos \theta & -\sin \theta \\ \sin \theta & \cos \theta \end{pmatrix} \begin{pmatrix} f_{\eta_8} & 0 \\ 0 & f_{\eta_1} \end{pmatrix}. \quad (3.14)$$

A general parameterization is proposed [109] by considering the  $U(1)_A$  anomaly [110],

$$\begin{pmatrix} f_\eta^8 & f_\eta^1 \\ f_{\eta'}^8 & f_{\eta'}^1 \end{pmatrix} = \begin{pmatrix} \cos \theta_8 & -\sin \theta_1 \\ \sin \theta_8 & \cos \theta_1 \end{pmatrix} \begin{pmatrix} f_{\eta_8} & 0 \\ 0 & f_{\eta_1} \end{pmatrix}. \quad (3.15)$$

Here  $\theta_1$  and  $\theta_8$  are actually two different mixing angle.

In order to show the  $SU(3)_F$  breaking, Feldmann, Kroll and Stech proposed to use the orthogonal flavor basis to describe the isoscalar meson states  $\eta^{(i)}$  [111].

$$\begin{pmatrix} |\eta\rangle \\ |\eta'\rangle \end{pmatrix} = \begin{pmatrix} \psi_\eta^q & \psi_\eta^s \\ \psi_{\eta'}^q & \psi_{\eta'}^s \end{pmatrix} \begin{pmatrix} |\eta_q\rangle \\ |\eta_s\rangle \end{pmatrix} = \begin{pmatrix} \cos \phi & -\sin \phi \\ \sin \phi & \cos \phi \end{pmatrix} \begin{pmatrix} \frac{1}{\sqrt{2}} |\bar{u}u + \bar{d}d\rangle \\ |\bar{s}s\rangle \end{pmatrix}. \quad (3.16)$$

The mixing angle in the flavor basis is related to the angle in the singlet-octet basis by  $\phi = \theta + \theta'$ , with  $\theta'$  being the rotation angle between the singlet-octet basis and the flavor basis ( $\cos \theta' = 1/\sqrt{3}$ ,  $\sin \theta' = \sqrt{2}/\sqrt{3}$ ). The decay constants of  $\eta^{(i)}$  and  $\eta_{q,s}$  defined via the orthogonal flavor currents  $J_{\mu 5}^{i=q} = (\bar{u}u + \bar{d}d) / \sqrt{2}$  and  $J_{\mu 5}^{i=s} = \bar{s}s$  are related by the same mixing matrix,

$$\begin{pmatrix} f_\eta^q & f_\eta^s \\ f_{\eta'}^q & f_{\eta'}^s \end{pmatrix} = \begin{pmatrix} \cos \phi & -\sin \phi \\ \sin \phi & \cos \phi \end{pmatrix} \begin{pmatrix} f_{\eta_q} & 0 \\ 0 & f_{\eta_s} \end{pmatrix}. \quad (3.17)$$

Transforming the flavor axial-vector currents into the single-octet currents, one obtain the relation between angles  $\theta_1$  and  $\theta_8$  proposed in Eq. (3.15)

$$\tan(\theta_1 - \theta_8) = \frac{\sqrt{2}}{3} \left( \frac{f_{\eta_s}}{f_{\eta_q}} - \frac{f_{\eta_q}}{f_{\eta_s}} \right). \quad (3.18)$$

In this sense, the two angles mixing scenario shown in Eq. (3.15) reveals the breaking of  $SU(3)_F$  symmetry.

When the TFFs evolve to large momentum transfers, one has to consider higher flavor state  $|\eta_c\rangle = |\bar{c}c\rangle$ . The mixing mechanism is then extended to  $\eta_q$ - $\eta_s$ - $\eta_c$  basis

$$\begin{pmatrix} f_\eta^q & f_\eta^s & f_\eta^c \\ f_{\eta'}^q & f_{\eta'}^s & f_{\eta'}^c \\ f_{\eta_c}^q & f_{\eta_c}^s & f_{\eta_c}^c \end{pmatrix} = \begin{pmatrix} \cos \phi & -\sin \phi & -\theta_c \sin \theta_y \\ \sin \phi & \cos \phi & \theta_c \cos \theta_y \\ -\theta_c \sin(\phi - \theta_c) & -\theta_c \cos(\phi - \theta_c) & 1 \end{pmatrix} \begin{pmatrix} f_{\eta_q} & 0 & 0 \\ 0 & f_{\eta_s} & 0 \\ 0 & 0 & f_{\eta_c} \end{pmatrix} \quad (3.19)$$

**Table 5.** Decay constants (GeV) and mixing angles (Degree) of flavor basis states. The default scale is 1 GeV for  $\eta_q$  and  $\eta_s$ , while 3 GeV for  $\eta_c$ .

$\mathcal{P}$	$f_{\mathcal{P}\text{-S1}}$ [111]	$f_{\mathcal{P}\text{-S2}}$ [112, 113]	$f_{\mathcal{P}\text{-S3}}$ [114]	$f_{\mathcal{P}\text{-Lattice}}$ [115]
$\eta_q$	$(1.07 \pm 0.02)f_\pi$	$(1.09 \pm 0.03)f_\pi$	$(1.08 \pm 0.04)f_\pi$	$0.09 \pm 0.01$
$\eta_s$	$(1.34 \pm 0.06)f_\pi$	$(1.66 \pm 0.06)f_\pi$	$(1.25 \pm 0.09)f_\pi$	$0.13 \pm 0.01$
$\phi$	$39.3 \pm 1.0$	$40.3 \pm 1.8$	$37.7 \pm 0.7$	$38.3 \pm 1.8$
$\eta_c$				$0.40 \pm 0.01$ [116]

**Table 6.** Masses (GeV) and the first two gegenbauer coefficients of the flavor basis states. The default scale is 1 GeV for  $\eta_q$  and  $\eta_s$ , while 3 GeV for  $\eta_c$ .

$\mathcal{P}$	$m_{\mathcal{P}\text{-S1}}$ [111]	$m_{\mathcal{P}\text{-S2}}$ [113]	$m_{\mathcal{P}\text{-S3}}$ [114]	$a_2^{\mathcal{P}}$ [117]	$a_4^{\mathcal{P}}$
$\eta_q$	0.11	0.31	0.21	$0.12 \pm 0.02$	—
$\eta_s$	0.71	0.72	0.71	$0.12 \pm 0.02$	—
$\eta_c$		2.98 [116]		0.13	0.04

Two new angles are introduced to relate the decay constants by  $f_\eta^c = -f_{\eta_c}\theta_c \sin\theta_y$  and  $f_{\eta'}^c = f_{\eta_c}\theta_c \cos\theta_y$ , in addition to  $f_{\eta_c}^c = f_{\eta_c}$ . We note that the  $\mathcal{O}(\theta_c^2)$  terms have been neglected in Eq. (3.19) since the mixing between light flavor basis and  $\eta_c$  is at  $\mathcal{O}(1/m_{\eta_c}^2)$ . So strictly speaking, the mixing matrix shown in Eq. (3.19) is not a unitary matrix  $UU^\dagger = 1 + \mathcal{O}(\theta_c^2)$ . Considering the axial vector anomaly at leading order, the three flavors mixing matrix is obtained in Ref. [111] as

$$U = \begin{pmatrix} \cos\phi & -\sin\phi & -0.006 \\ \sin\phi & \cos\phi & -0.016 \\ 0.015 & 0.008 & 1 \end{pmatrix}. \quad (3.20)$$

Here the angle  $\theta_c = -1.0^\circ$  and the decay constants  $f_\eta^c = -2.4$  MeV,  $f_{\eta'}^c = -6.3$  MeV are indicated.

The  $\eta^{(\prime)}$  TFFs are then expressed in terms of TFFs of flavor basis states as

$$\begin{aligned} \mathcal{F}_{\eta\gamma\gamma^*} &= \cos\phi \frac{e_u^2 + e_d^2}{\sqrt{2}} \mathcal{F}_{\eta_q\gamma\gamma^*} - \sin\phi e_s^2 \mathcal{F}_{\eta_s\gamma\gamma^*} - 0.006 e_c^2 \mathcal{F}_{\eta_c\gamma\gamma^*}, \\ \mathcal{F}_{\eta'\gamma\gamma^*} &= \sin\phi \frac{e_u^2 + e_d^2}{\sqrt{2}} \mathcal{F}_{\eta_q\gamma\gamma^*} + \cos\phi e_s^2 \mathcal{F}_{\eta_s\gamma\gamma^*} - 0.016 e_c^2 \mathcal{F}_{\eta_c\gamma\gamma^*}. \end{aligned} \quad (3.21)$$

The first and second terms can be obtained directly by substituting the the flavor basis states  $\eta_q$  and  $\eta_s$  into  $\mathcal{F}_{\mathcal{P}\gamma\gamma^*}$  expressed in Eq. (3.9). In table 5 we collect the decay constants of different flavor basis states. The results in the first row, denoted by S1, S2 and S3, are obtained from different phenomenological analysis. We also list the recent lattice QCD result [115], which is much smaller than the result obtained in S1, S2 and S3 when we

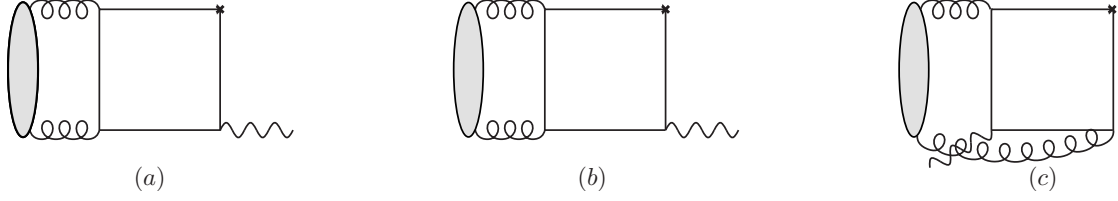


**Figure 11.** The contribution to  $\eta^{(\prime)}$  TFF from the  $|gg\rangle$  state.

take  $f_\pi = 0.13$  GeV. For the charmonium state, we take the lattice evaluation  $f_{\eta_c} = 0.40 \pm 0.10$  GeV by considering both the QCD and QED contributions [116]. In table 6 we list the masses and the first two gegenbauer moments of flavor basis states. We chose  $a_2^{\mathcal{P}}(2 \text{ GeV}) = 0.09 \pm 0.02$  from the RQCD collaboration. Actually, what they studied is the  $SU(3)$  octet  $a_2^{\eta_8}$  [117], and here we assume that the  $SU(3)$  breaking appears only in the difference of decay constants.

The third term in Eq. (3.21) comes from the  $\eta_c$  TFF

$$\begin{aligned}
\mathcal{F}_{\eta_c \gamma \gamma^*}(Q^2) &= e_c^2 \int_0^1 du \int bdb e^{-S} S_t f_{\eta_c} \\
&\cdot \left\{ 2\varphi(u) \hat{\Sigma}(u, b) K_0(\kappa'_1 b) + g_2(u) \left[ \frac{2ub}{\kappa'_1} K_1(\kappa'_1 b) - \frac{2\bar{u}b}{\kappa'_2} K_1(\kappa'_2 b) \right] \right. \\
&\quad - g_1(u) \left[ \frac{2b}{\kappa'_1} K_1(\kappa'_1 b) + \frac{2b}{\kappa'_2} K_1(\kappa'_2 b) \right] \\
&\quad - g_1(u) \left[ \frac{b^2 m_c^2}{\kappa_1'^2} K_2(\kappa'_1 b) + \frac{b^2 m_c^2}{\kappa_2'^2} K_2(\kappa'_2 b) \right] \\
&\quad + \tilde{g}_2(u) \left[ \frac{2b}{\kappa'_1} K_1(\kappa'_1 b) - \frac{2b}{\kappa'_2} K_1(\kappa'_2 b) \right] \\
&\quad \left. + \tilde{g}_2(u) \left[ \frac{b^2 m_c^2}{\kappa_1'^2} K_2(\kappa'_1 b) - \frac{b^2 m_c^2}{\kappa_2'^2} K_2(\kappa'_2 b) \right] \right\}. \tag{3.22}
\end{aligned}$$

The auxiliary function  $\tilde{g}_2(u) = \int_0^u du' g_2(u') / (p_1 \cdot z_1)$  is called in the analysis. The virtualities are  $\kappa'_1 = [uQ^2 + m_c^2]^{1/2}$  and  $\kappa'_2 = [\bar{u}Q^2 + m_c^2]^{1/2}$ . In addition to the virtualities, charm quark mass give another power correction terms  $\mathcal{O}(b/\kappa_{1,2})$  to the hard kernel associated the LCDAs  $g_1$  and  $\tilde{g}_2$ , here  $b$  is a dimensionless transversal parameter. Eq. (3.22) show the result accompanying with the valence quark state. In the numerics, we only take into account the leading twist contribution, since the high twist LCDAs are not understood well so far. The transversal size parameter of  $\eta_c$  is chosen at  $\beta_{\eta_c}^2 = 0.19 \text{ GeV}^{-2}$  from the phenomenological analysis of two-photon decay width  $\Gamma(\eta_c \rightarrow \gamma\gamma)$  [102].

We do not take in to account the  $|gg\rangle$  component in  $\eta^{(\prime)}$ . Actually, this component define another leading twist LCDAs. However, the asymptotic term of gluon LCDAs vanishes due to the charge conjugate symmetry, and its contribution comes from the non-perturbative correction terms proportional to the gegenbauer polynomials  $C_n^{5/2}(2u - 1)$ . In addition, the  $|gg\rangle$  state contributes to the TFFs at NLO with a hard coupling scale, as

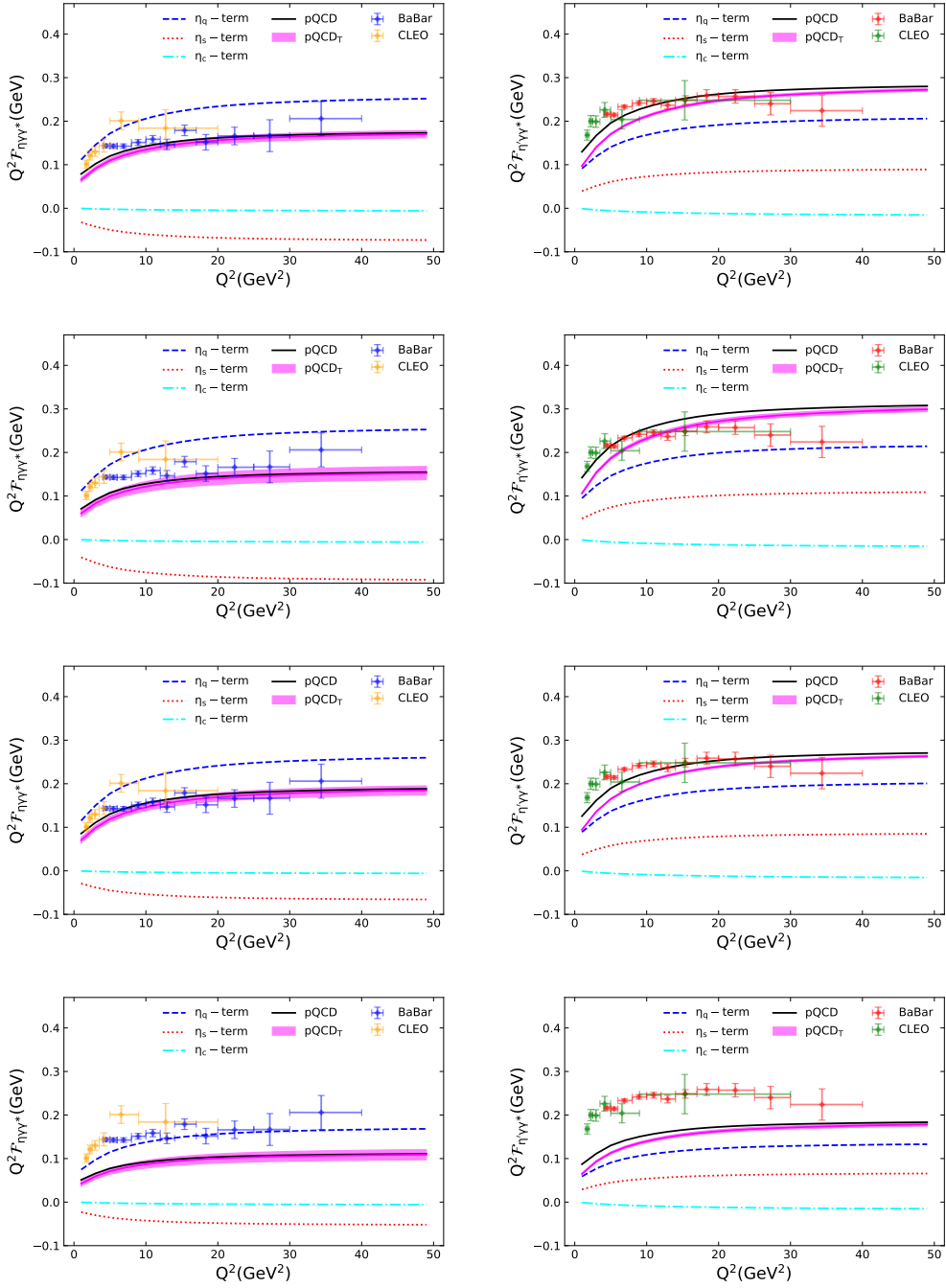


**Figure 12.** The pQCD predictions of  $\eta$  (left) and  $\eta'$  (right) TFFs in the momentum transfers  $Q^2 \leq 50 \text{ GeV}^2$ .

shown in figure 11, hence its contribution is formally at the order of  $\mathcal{O}(\alpha_s)$ . In conclusion, the contribution to  $\eta^{(\prime)}$  TFF from the valence gluon state is doubly suppressed by the strong coupling and the gegenbauer expansion.

We depict the pQCD predictions of  $\eta^{(\prime)}$  TFFs in figure 12. The contributions from

$\eta_q$ ,  $\eta_s$  and  $\eta_c$  components and their sum are shown in the blue-dashed, red-dotted, cyan-dashing and black-thick curves, respectively, the iTMD-improved pQCD prediction is shown in magenta band. We plot the TFFs by considering all the four mixing schemes collected in table 5 and table 6. We find that

- (1) TFFs of  $\eta$  and  $\eta'$  mesons are dominated by  $\eta_q$  component, meanwhile, TFF of  $\eta'$  meson also receive comparable contribution from the  $\eta_s$  component.
- (2) The contribution from  $\eta_c$  component is tiny in magnitude, hence do not play important role in the explanation of data.
- (3) The iTMD-improved pQCD predictions favor the small mixing angle, the large decay constants and the small masses of flavor basis states, denoted by S1 and S3.

In the perturbative QCD limit, TFFs of different flavor basis states are equal to each other  $\mathcal{F}_{\eta_q\gamma\gamma^*} = \mathcal{F}_{\eta_s\gamma\gamma^*} = \mathcal{F}_{\eta_c\gamma\gamma^*} = \mathcal{F}_{\pi\gamma\gamma^*}$ , we then have the asymptotic relation for the difference between  $\eta$  and  $\eta'$  TFFs from Eqs. (3.21).

$$\delta\mathcal{F} \equiv \mathcal{F}_{\eta\gamma\gamma^*} - \mathcal{F}_{\eta'\gamma\gamma^*} \xrightarrow{Q^2 \rightarrow \infty} (0.071 \pm 0.032) \sqrt{2} f_\pi = 0.013 \pm 0.006. \quad (3.23)$$

The uncertainty mainly comes from the mixing angle  $\phi = 39.6^\circ \pm 2.6^\circ$ . This relation can be compared to the BABAR result at the energy point  $Q^2 = 112 \text{ GeV}^2$ , saying  $\delta\mathcal{F}(Q^2 = 112 \text{ GeV}^2) = 0.25_{-0.02}^{+0.02} - 0.23_{-0.03}^{+0.03} = 0.02 \pm 0.02$  [100], but keep in mind of the uncertainty from data. We find that this observable is sensitive to the mixing angle, so we suggest the further precise measurement at an ultraviolet momentum transfer  $Q^2 \sim \mathcal{O}(10^2) \text{ GeV}^2$  to determine the this important parameter and hence to specify the mixing mechanism.

## 4 Summary

We systematically study the EMFFS and TFFs of light pseudoscalar mesons ( $\pi$ ,  $K$ ,  $\eta^{(\prime)}$ ) from the perturbative QCD approach based on  $k_T$  factorization. The predictions are obtained at next-to-leading-order QCD correction  $\mathcal{O}(\alpha_s^2)$  for the leading and sub-leading twist LCDAs, and at leading order  $\mathcal{O}(\alpha_s)$  for the twist four LCDAs. In order to include the soft transversal degree of freedom in the parton distribution of hadrons, we introduce the iTMDs, supplementing to the LCDAs which describes the soft longitudinal degree of freedom inside the hadrons. The main motivation is that the initial and final hadrons are formed outside the hard interaction scope, where the suppression of the small transversal momentum from the sudakov exponent is weak, hence the partons inside hadrons show an oscillation in the transversal plane, orthogonal to the light-cone direction.

Due to the chiral enhancement, EMFFs of pion and kaon mesons are dominated by the twist three LCDAs associated to the valence quark state, which is proportional to the chiral mass. The transversal-size parameters of pion meson is obtained at  $\beta_\pi^2 = 0.51 \pm 0.04 \text{ GeV}^{-2}$  with the double photon radiation relation and the current understanding of

gegenbauer coefficients. With the iTMDs-improved pQCD calculation of spacelike pion EMFFs and the result obtained from the modular dispersion relation with the timelike measurement and pQCD high energy tail, we fit the chiral mass of pion meson and obtain  $m_0^\pi(1 \text{ GeV}) = 1.84 \pm 0.07 \text{ GeV}$ . This value is thirty percents larger than the previous pQCD result, but consists with the ChPT, indicating a sizable decrease of form factor due to the soft transversal dynamics, especially in the small and intermediate momentum transfers.

For the EMFFs of kaon meson, thanks to the abundant data in the timelike region with large momentum transfers where the perturbative QCD holds well, we can fit the iTMDs-improved pQCD calculation directly to the data. We then obtain the transversal-size parameter  $\beta_K^2 = 0.30 \pm 0.05 \text{ GeV}^{-2}$  by taking the well-known chiral relation of chiral mass  $m_0^K(1 \text{ GeV}) = 1.90 \text{ GeV}$ . This value is smaller than the result of pion, revealing a sizable  $SU(3)$  flavor violating and a stronger attracting between the strange and light quarks system. The improved pQCD prediction of spacelike form factor shows a good consistent with the next-to-next-to-leading-order calculation from collinear factorization, although the results from QCD calculations are small in comparing to the lattice evaluation. We mark that this difference may be accounted by the strange quark effect in the kaon LCDAs which decreases the pQCD prediction by about thirty percents.

The meson-photon TFFs are also affected by the iTMDs in the small and intermediate momentum transfers. The improved pQCD prediction favors the Belle data of pion-photon TFF which shows a stable  $Q^2 F_{\pi\gamma\gamma^*}$  in the large momentum transfers. Since this form factor is sensitive to the leading twist LCDAs, we hope the further measurement from Belle-II would help us to determine the gegenbauer coefficients of pion, for which the current result obtained from lattice evaluations and QCD-based analysis show some differences. For the TFFs of  $\eta$  and  $\eta'$  mesons, we do the pQCD calculations under the flavor basis mixing scheme ( $\eta_q$ - $\eta_s$ - $\eta_c$ ) with considering four different sets of parameters. The result shows a small contribution from the charmonium basis, and dominate contribution from  $\eta_q$  state for  $\eta$  and  $\eta'$  TFFs. In addition, our prediction prefers the small mixing angle, the large decay constants and the small masses of flavor basis states  $\eta_q$  and  $\eta_s$ . We suggest the measurement of  $\mathcal{F}_{\eta\gamma\gamma^*}$  and  $\mathcal{F}_{\eta'\gamma\gamma^*}$  at an ultraviolet  $Q^2 \sim \mathcal{O}(10^2) \text{ GeV}^2$  since their difference is very sensitive to the mixing angle.

## 5 ACKNOWLEDGEMENTS

We are grateful to Vladimir Braun, Heng-tong Ding, Jun Hua, Guang-shun Huang, Hsiang-nan Li, Wei Wang and Yu-ming Wang for fruitful discussions. This work is supported by the National Key R&D Program of China under Contracts No. 2023YFA1606000 and the National Science Foundation of China (NSFC) under Grant No. 11975112. J. C is also supported by the Launching Funding of Henan University of Technology (No.31401697).



## A Definition of the light-cone distribution amplitudes

Light-cone distribution amplitudes (LCDAs) are probability amplitudes to find the hadron in a state with certain number of fock constituents at small transversal separation. They are usually studied by applying the conformal symmetry in QCD [118]. The underlying idea is somewhat like the partial-wave expansion in quantum mechanism where the angular degree of freedom (dof) is detached from the radial one for a spherically symmetric potential. For the LCDAs, the transversal and longitudinal dofs are separated after considering the invariance of massless QCD under the conformal transformation. The transversal momentum dependence is governed by the renormalization group equations which show a scale dependence on the ultraviolet cutoff  $\mu$ . The dependence on the longitudinal momentum fractions is governed in terms of orthogonal Jacobi polynomials which deduces to the Gegenbauer polynomials representing the so-called collinear subgroup of the conformal group [9]. In addition, the distributions with different conformal spins ( $j = (l + s/2$  with  $l$  being the canonical dimension and  $s$  being the lorentz spin projection) have independently behaviors [119].

LCDAs of pseudoscalar meson ( $\mathcal{P} = \pi$  and  $K$ ) with the valence quark state is defined via the nonlocal matrix element [120, 121].

$$\begin{aligned} \langle 0 | \bar{u}(z_2) (\gamma_\rho \gamma_5) q(z_1) | \mathcal{P}^-(p) \rangle &= f_{\mathcal{P}} \int_0^1 du e^{-iupz_1 - i\bar{u}pz_2} \left\{ ip_\rho [\varphi(u, \mu) \right. \\ &\quad \left. + (z_1 - z_2)^2 g_1(u, \mu)] + \left[ (z_1 - z_2)_\rho - \frac{p_\rho (z_1 - z_2)^2}{p(z_1 - z_2)} \right] g_2(u, \mu) \right\}, \end{aligned} \quad (\text{A.1})$$

$$\begin{aligned} \langle 0 | \bar{u}(z_2) (\sigma_{\tau\tau'} \gamma_5) q(z_1) | \mathcal{P}^-(p) \rangle &= f_{\mathcal{P}} m_0^{\mathcal{P}} \int_0^1 dx e^{-iupz_1 - i\bar{u}pz_2} \left( 1 - \frac{m_{\mathcal{P}}^2}{(m_0^{\mathcal{P}})^2} \right) \\ &\quad \cdot \left[ p^\tau (z_1 - z_2)_{\tau'} - p^{\tau'} (z_1 - z_2)_\tau \right] \varphi^\sigma(u, \mu), \end{aligned} \quad (\text{A.2})$$

$$\langle 0 | \bar{u}(z_2) (i\gamma_5) q(z_1) | \mathcal{P}^-(p) \rangle = f_{\mathcal{P}} m_0^{\mathcal{P}} \int_0^1 du e^{-iupz_1 - i\bar{u}pz_2} \varphi^p(u, \mu). \quad (\text{A.3})$$

Here  $\varphi$ ,  $\varphi^{P,\sigma}$  and  $g_{1,2}$  corresponds to the leading twist, twist three and twist four LCDAs, respectively. The twist is defined by the minus between canonical dimension and spin projection  $t = l - s$ .  $f_{\mathcal{P}}$  is the decay constant and  $m_0^{\mathcal{P}} \equiv \frac{m_{\mathcal{P}}^2}{m_u + m_q}$  is the chiral mass.

For the high fock state with  $\bar{q}qg$  assignment, the LCDAs are defined via the matrix elements with the gluon field strength tensor operator  $G_{\kappa\kappa'} = g_s G_{\kappa\kappa'}^a \lambda^a / 2$ ,

$$\begin{aligned} p^+ \langle 0 | \bar{u}(z_2) (\sigma_{\tau\tau'} \gamma_5) G_{\kappa\kappa'}(z_0) q(z_1) | \mathcal{P}^-(p) \rangle &= if_{3\mathcal{P}} \int \mathcal{D}x_i e^{-i\alpha_1 pz_1 - i\alpha_2 pz_2 - i\alpha_3 z_0} \\ &\quad \cdot \left[ (p_\kappa p_\tau g_{\kappa'\tau'} - p_{\kappa'} p_\tau g_{\kappa\tau'}) - (p_\kappa p_{\tau'} g_{\kappa'\tau} - p_{\kappa'} p_{\tau'} g_{\kappa\tau}) \right] \varphi_3(\alpha_i, \mu), \end{aligned} \quad (\text{A.4})$$

$$\begin{aligned} p^+ \langle 0 | \bar{u}(z_2) (\gamma_\rho \gamma_5) G_{\kappa\kappa'}(z_0) q(z_1) | \mathcal{P}^-(p) \rangle &= f_{\mathcal{P}} \int \mathcal{D}x_i e^{-i\alpha_1 pz_1 - i\alpha_2 pz_2 - i\alpha_3 z_0} \\ &\quad \cdot \left[ p_\rho \frac{p_\kappa (z_1 - z_2)_{\kappa'} - p_{\kappa'} (z_1 - z_2)_\kappa}{p(z_1 - z_2)} \varphi_{\parallel}(\alpha_i, \mu) + (g_{\rho\kappa}^\perp p_{\kappa'} - g_{\rho\kappa'}^\perp p_\kappa) \varphi_{\perp}(\alpha_i, \mu) \right], \end{aligned} \quad (\text{A.5})$$

$$p^+ \langle 0 | \bar{u}(z_2) (\gamma_\rho) \tilde{G}_{\kappa\kappa'}(z_0) q(z_1) | \mathcal{P}^-(p) \rangle = f_{\mathcal{P}} \int \mathcal{D}x_i e^{-i\alpha_1 p z_1 - i\alpha_2 p z_2 - i\alpha_3 z_0} \cdot \left[ p_\rho \frac{p_\kappa(z_1 - z_2)_{\kappa'} - p_{\kappa'}(z_1 - z_2)_\kappa}{p(z_1 - z_2)} \tilde{\varphi}_{\parallel}(\alpha_i, \mu) + (g_{\rho\kappa}^\perp p_{\kappa'} - g_{\rho\kappa'}^\perp p_\kappa) \tilde{\varphi}_{\perp}(\alpha_i, \mu) \right]. \quad (\text{A.6})$$

Here  $\varphi_{3\mathcal{P}}$  is the twist-3 DA, and  $\varphi_{\parallel,\perp}, \tilde{\varphi}_{\parallel,\perp}$  are twist-4 DAs,  $\tilde{G}_{\kappa\kappa'} = 1/2 \epsilon_{\kappa\kappa'\eta\eta'} G^{\eta\eta'}$  is the dual gluon-field-strength tensor at the location  $z_0 = v z_1 + \bar{v} z_2$  with the free variable  $v \in [0, 1]$ . The integration measure is

$$\int \mathcal{D}\underline{\alpha} = \int_0^1 d\alpha_1 d\alpha_2 d\alpha_3 \delta(1 - \alpha_1 - \alpha_2 - \alpha_3). \quad (\text{A.7})$$

## B Expressions of the light-cone distribution amplitudes

For the pseudoscalar meson without polarisation, the leading twist LCDA is written in terms of Gegenbauer polynomials as

$$\varphi(u, \mu) = 6u\bar{u} \sum_{n=0} a_n(\mu) C_n^{3/2}(2u - 1). \quad (\text{B.1})$$

Two-particle twist-3 DAs are related to the three-particle DA  $\varphi_3(\alpha_i)$  by the QCD equation of motion (EOM). The EOM relations contain the quark mass terms which are subsequently written by means of two dimensionless parameters  $\rho_+^{\mathcal{P}} = (m_q + m_u)/m_0^{\mathcal{P}}$  and  $\rho_-^{\mathcal{P}} = (m_q - m_u)/m_0^{\mathcal{P}}$ . We take into account the strange quark mass in the calculation, and neglect the  $u, d$  quark masses unless in the chiral masses  $m_0^{\mathcal{P}}$ . To the next-to-leading-order definition of conformal spin and to the second moments in the truncated conformal expansion, we get

$$\begin{aligned} \varphi^p(u, \mu) = & 1 + 3\rho_+^{\mathcal{P}}(1 + 6a_2) - 9\rho_-^{\mathcal{P}}a_1 + \left[ \frac{27}{2}\rho_+^{\mathcal{P}}a_1 - \rho_-^{\mathcal{P}} \left( \frac{3}{2} + 27a_2 \right) \right] C_1^{1/2}(2u - 1) \\ & + [30\eta_3 + 15\rho_+^{\mathcal{P}}a_2 - 3\rho_-^{\mathcal{P}}a_1] C_2^{1/2}(2u - 1) + \left[ 10\eta_3\lambda_3 - \frac{9}{2}\rho_-^{\mathcal{P}}a_2 \right] C_3^{1/2}(2u - 1) \\ & - 3\eta_3\omega_3 C_4^{1/2}(2u - 1) + \frac{3}{2}(\rho_+^{\mathcal{P}} + \rho_-^{\mathcal{P}}) (1 - 3a_1 + 6a_2) \ln u \\ & + \frac{3}{2}(\rho_+^{\mathcal{P}} - \rho_-^{\mathcal{P}}) (1 + 3a_1 + 6a_2) \ln \bar{u}, \end{aligned} \quad (\text{B.2})$$

$$\begin{aligned} \varphi^\sigma(u, \mu) = & 6u\bar{u} \left\{ 1 + \frac{5}{2}\rho_+^{\mathcal{P}} + 15\rho_+^{\mathcal{P}}a_2 - \frac{15}{2}\rho_-^{\mathcal{P}}a_1 + \left[ 3\rho_+^{\mathcal{P}}a_1 - \frac{15}{2}\rho_-^{\mathcal{P}}a_2 \right] C_1^{3/2}(2u - 1) \right. \\ & + \left[ 5\eta_3 - \frac{1}{2}\eta_3\omega_3 + \frac{3}{2}\rho_+^{\mathcal{P}}a_2 \right] C_2^{3/2}(2u - 1) + \eta_3\lambda_3 C_3^{3/2}(2u - 1) \\ & \left. + \frac{3}{2}(\rho_+^{\mathcal{P}} + \rho_-^{\mathcal{P}}) (1 - 3a_1 + 6a_2) \ln u + \frac{3}{2}(\rho_+^{\mathcal{P}} - \rho_-^{\mathcal{P}}) (1 + 3a_1 + 6a_2) \ln \bar{u} \right\} \end{aligned} \quad (\text{B.3})$$

$$\varphi_3(\alpha_i, \mu) = 360\alpha_1\alpha_2\alpha_3^2 \left\{ 1 + \lambda_3(\alpha_1 - \alpha_2) + \omega_3 \frac{1}{2}(7\alpha_3 - 3) \right\}. \quad (\text{B.4})$$

The asymptotic term, the terms from EOM and the  $\bar{q}qg$  operators are clearly separated in the above expressions. The three-particle parameters  $f_{3\mathcal{P}}, \lambda_3, \omega_3$  can be defined by the matrix element of local twist-3 operators, and their evolution have the mixing terms with the quark mass [120].

For the two-particle twist-4 DAs, the gauge invariant and lorentz invariant definition in Eq. (A.1) is more convenient to be used in the QCD calculation. They are related to the invariant amplitudes  $\psi_{4\mathcal{P}}, \phi_{4\mathcal{P}}$  by

$$g_2(u, \mu) = -\frac{1}{2} \int_0^u du' \psi_4(u'), \quad g_1(u, \mu) = \frac{1}{16} \phi_4(u) + \int_0^u du' g_2(u'). \quad (\text{B.5})$$

The relations between different operators by EOM indicate that the lorentz invariant amplitudes are written in terms of the "genuine" twist-4 contribution from the three-particle DAs  $\varphi_{\parallel}(\alpha_i), \varphi_{\perp}(\alpha_i)$  and the Wandzura-Wilczek-type mass corrections from the two-particle lower twist DAs, distinguishing by parameters  $\delta_{\mathcal{P}}^2$  and  $m_{\mathcal{P}}^2$ , respectively [125].

$$\begin{aligned} \psi_4(u, \mu) = & \delta_{\mathcal{P}}^2 \left[ \frac{20}{3} C_2^{1/2}(2u-1) + \frac{49}{2} a_1 C_3^{1/2}(2u-1) \right] \\ & + m_{\mathcal{P}}^2 \left\{ 6\rho^{\mathcal{P}} (1-3a_1+6a_2) C_0^{1/2}(2u-1) \right. \\ & - \left[ \frac{18}{5} a_1 + 3\rho^{\mathcal{P}} (1-9a_1+18a_2) + 12\kappa_4 \right] C_1^{1/2}(2u-1) \\ & + \left[ 2-6\rho^{\mathcal{P}} (a_1-5a_2) + 60\eta_3 \right] C_2^{1/2}(2u-1) \\ & + \left( \frac{18}{5} a_1 - 9\rho^{\mathcal{P}} a_2 + \frac{16}{3} \kappa_4 + 20\eta_3 \lambda_3 \right) C_3^{1/2}(2u-1) \\ & \left. + \left( \frac{9}{4} a_2 - 6\eta_3 \omega_3 \right) C_4^{1/2}(2u-1) \right\} + 6m_q^2 (1-3a_1+6a_2) \ln u, \end{aligned} \quad (\text{B.6})$$

$$\begin{aligned} \phi_4(u, \mu) = & \delta^2 \left\{ \left( \frac{200}{3} + 196(2x-1)a_1 \right) u^2 \bar{u}^2 \right. \\ & + 21\omega_4 (u\bar{u}(2+13u\bar{u}) + [2u^3(6u^2-15u+10) \ln u] + [u \leftrightarrow \bar{u}]) \\ & - 14a_1 (u\bar{u}(2u-1)(2-3u\bar{u}) - [2u^3(u-2) \ln u] + [u \leftrightarrow \bar{u}]) \left. \right\} \\ & + m_{\mathcal{P}}^2 \left\{ \frac{16}{3} \kappa_4 (u(2u-\bar{u})(1-2u\bar{u}) + [5(u-2)u^3 \ln u] - [u \leftrightarrow \bar{u}]) \right. \\ & + 4\eta_3 u\bar{u} \left[ 60\bar{u} + 10\lambda_3 ((2u-1)(1-u\bar{u}) - (1-5u\bar{u})) \right. \\ & - \left. \omega_3 (3-21u\bar{u} + 28u^2\bar{u}^2 + 3(2u-1)(1-7u\bar{u})) \right] \\ & - \frac{36}{5} a_2 \left( \frac{1}{4} u\bar{u}(4-9u\bar{u} + 110u^2\bar{u}^2) + [u^3(10-15u+6u^2) \ln u] + [u \leftrightarrow \bar{u}] \right) \\ & \left. + 4u\bar{u}(1+3u\bar{u}) \left( 1 + \frac{9}{5} (2u-1)a_1 \right) \right\}. \end{aligned} \quad (\text{B.7})$$

Here  $\eta_3 = f_{3\mathcal{P}}/(f_{\mathcal{P}}m_0^{\mathcal{P}})$ . It is noticed in Eq. (B.6) that  $\psi_4(u)$  has a logarithm end-point singularity for the finite quark mass, while this singularity is not existed in  $\phi_4(u)$ . Three-

particle twist-4 DAs read as

$$\begin{aligned} \psi_{\parallel}(\alpha_i, \mu) &= 120\alpha_1\alpha_2\alpha_3 \left\{ \delta^2 \left[ \frac{21}{8}(\alpha_1 - \alpha_2)\omega_4 + \frac{7}{20}a_1(1 - 3\alpha_3) \right] \right. \\ &\quad \left. + m^2 \left[ -\frac{9}{20}(\alpha_1 - \alpha_2)a_2 + \frac{1}{3}\kappa_4 \right] \right\}, \end{aligned} \quad (\text{B.8})$$

$$\begin{aligned} \psi_{\perp}(\alpha_i, \mu) &= 30\alpha_3^2 \left\{ \delta^2 \left[ \frac{1}{3}(\alpha_1 - \alpha_2) + \frac{7}{10}a_1 \left( -\alpha_3(1 - \alpha_3) + 3(\alpha_1 - \alpha_2)^2 \right) \right] \right. \\ &\quad \left. + \frac{21}{4}\omega_4(\alpha_1 - \alpha_2)(1 - 2\alpha_3) \right] + m^2(1 - \alpha_3) \left[ \frac{9}{40}(\alpha_1 - \alpha_2) - \frac{1}{3}\kappa_4 \right] \right\}, \end{aligned} \quad (\text{B.9})$$

$$\tilde{\psi}_{\parallel}(\alpha_i, \mu) = -120\alpha_1\alpha_2\alpha_3\delta^2 \left\{ \frac{1}{3} + \frac{7}{4}a_1(\alpha_1 - \alpha_2) + \frac{21}{8}\omega_4(1 - 3\alpha_3) \right\}, \quad (\text{B.10})$$

$$\begin{aligned} \tilde{\psi}_{\perp}(\alpha_i, \mu) &= 30\alpha_3^2 \left\{ \delta^2 \left[ \frac{1}{3}(1 - \alpha_3) - \frac{7}{10}a_1(\alpha_1 - \alpha_2)(4\alpha_3 - 3) + \frac{21}{4}\omega_4(1 - \alpha_3)(1 - 2\alpha_3) \right] \right. \\ &\quad \left. + m^2 \left[ \frac{9}{40}a_2(\alpha_1^2 - 4\alpha_1\alpha_2 + \alpha_2^2) - \frac{1}{3}(\alpha_1 - \alpha_2)\kappa_4 \right] \right\}. \end{aligned} \quad (\text{B.11})$$

Three nonperturbative parameters  $\delta^2, \omega_4$  are introduced. We mark that all parameters in the conformal expansion of DAs have the scale dependence and the behaviours of their evolutions can be found in Ref. [120].

## C A Derivation of the modulus squared dispersion relation

In order to derive the modulus squared dispersion relation shown in Eq. (2.31), we firstly introduce an auxiliary  $g_{\pi}$  function

$$g_{\pi}(q^2) \equiv \frac{\ln F_{\pi}(q^2)}{q^2 \sqrt{s_0 - q^2}}. \quad (\text{C.1})$$

The only assumption in our derivation is that the form factor  $F_{\pi}(q^2)$  is free of zeros in the complex  $q^2$  plane, then the  $g_{\pi}$  function has no additional singularities in the  $q^2$  plane, apart from the region  $q^2 = s > s_0$  on the real axis. The normalization condition  $F_{\pi}(0) = 1$  indicates that  $g_{\pi}(0)$  is finite. What's more, the power asymptotics of pion form factor  $F_{\pi}(q^2) \sim 1/q^2$  implies  $g_{\pi}(q^2) \sim 1/(q^2)^{\alpha}$  at  $|q^2| \rightarrow \infty$  with the parameter  $\alpha > 1$ , which enables a dispersion relation for the  $g_{\pi}$  function

$$g_{\pi}(q^2) = \frac{1}{\pi} \int_{s_0}^{\infty} ds \frac{\text{Im } g_{\pi}(s)}{s - q^2 - i\epsilon}. \quad (\text{C.2})$$

The derivation of Eq. (C.2) is in the same way as for the standard dispersion relation of pion form factor shown in Eq. (2.30).

At  $s > s_0$  on the real axis, the imaginary part of  $g_{\pi}$  reads as

$$\text{Im } g_{\pi}(s) = \text{Im} \left[ \frac{\ln(|F_{\pi}(s)|e^{i\delta_{\pi}(s)})}{-is\sqrt{s - s_0}} \right] = \frac{\ln |F_{\pi}(s)|}{s\sqrt{s - s_0}}, \quad (\text{C.3})$$

where the pion form factor is written by  $F_\pi(s) = |F_\pi(s)|e^{i\delta_\pi(s)}$  and the branch point is chosen at  $\sqrt{s_0 - (s + i\epsilon)} \xrightarrow{\epsilon \rightarrow 0} -i\sqrt{s - s_0}$ . We note that the other branch point  $+i\sqrt{s - s_0}$  would lead to an unphysical divergence of the pion form factor, saying  $F_\pi(q^2) = \infty$  at  $q^2 \rightarrow -\infty$ .

Substituting Eq. (C.1) and Eq. (C.3) into the dispersion relation Eq. (C.2), we get

$$\frac{\ln F_\pi(q^2)}{q^2 \sqrt{s_0 - q^2}} = \frac{1}{2\pi} \int_{s_0}^{\infty} \frac{ds \ln |F_\pi(s)|^2}{s \sqrt{s - s_0} (s - q^2)}, \quad q^2 < s_0. \quad (\text{C.4})$$

Taking exponent to the both sides, we arrive at the modulus squared dispersion relation

$$F_\pi(q^2) = \exp \left[ \frac{q^2 \sqrt{s_0 - q^2}}{2\pi} \int_{s_0}^{\infty} \frac{ds \ln |F_\pi(s)|^2}{s \sqrt{s - s_0} (s - q^2)} \right]. \quad (\text{C.5})$$

## References

- [1] A. H. Mueller, Phys. Rept. **73**, 237 (1981)
- [2] S.J. Brodsky, G.P. Lepage, in: A.H. Mueller (Ed.), *Perturbative Quantum Chromodynamics*, World Scientific, Singapore, 1989
- [3] A. V. Efremov and A. V. Radyushkin, Phys. Lett. B **94**, 245-250 (1980)
- [4] G. P. Lepage and S. J. Brodsky, Phys. Rev. D **22**, 2157 (1980)
- [5] M. Diehl, Phys. Rept. **388**, 41-277 (2003)
- [6] A. V. Belitsky and A. V. Radyushkin, Phys. Rept. **418**, 1-387 (2005)
- [7] V. M. Braun and I. E. Filyanov, Z. Phys. C **48**, 239-248 (1990)
- [8] P. Ball, V. M. Braun and A. Lenz, JHEP **05**, 004 (2006)
- [9] P. Ball, V. M. Braun, Y. Koike and K. Tanaka, Nucl. Phys. B **529**, 323-382 (1998)
- [10] P. Ball and V. M. Braun, Nucl. Phys. B **543**, 201-238 (1999)
- [11] P. Ball and G. W. Jones, JHEP **03**, 069 (2007)
- [12] P. Ball, V. M. Braun and A. Lenz, JHEP **08**, 090 (2007)
- [13] V. Braun, R. J. Fries, N. Mahnke and E. Stein, Nucl. Phys. B **589**, 381-409 (2000) [erratum: Nucl. Phys. B **607**, 433-433 (2001)]
- [14] Y. L. Zhang, S. Cheng, J. Hua and Z. J. Xiao, Phys. Rev. D **92**, no.9, 094031 (2015)
- [15] Y. L. Shen, Z. T. Zou and Y. Li, Phys. Rev. D **100**, no.1, 016022 (2019)
- [16] H. Zhou, J. Yan, Q. Yu and X. G. Wu, Phys. Rev. D **108**, no.7, 074020 (2023)
- [17] S. V. Mikhailov, A. V. Pimikov and N. G. Stefanis, Phys. Rev. D **103**, no.9, 096003 (2021)
- [18] J. Gao, T. Huber, Y. Ji and Y. M. Wang, Phys. Rev. Lett. **128**, no.6, 6 (2022)

- [19] A. Gérardin, H. B. Meyer and A. Nyffeler, Phys. Rev. D **94**, no.7, 074507 (2016)
- [20] V. M. Braun, A. Khodjamirian and M. Maul, Phys. Rev. D **61**, 073004 (2000)
- [21] J. Bijnens and A. Khodjamirian, Eur. Phys. J. C **26**, 67-79 (2002)
- [22] S. Cheng, A. Khodjamirian and A. V. Rusov, Phys. Rev. D **102**, no.7, 074022 (2020)
- [23] H. n. Li, Y. L. Shen, Y. M. Wang and H. Zou, Phys. Rev. D **83**, 054029 (2011)
- [24] S. Cheng, Y. Y. Fan and Z. J. Xiao, Phys. Rev. D **89**, no.5, 054015 (2014)
- [25] H. C. Hu and H. n. Li, Phys. Lett. B **718**, 1351-1357 (2013)
- [26] S. Cheng and Z. J. Xiao, Phys. Lett. B **749** (2015), 1-7
- [27] S. Cheng, Phys. Rev. D **100**, no.1, 013007 (2019)
- [28] L. B. Chen, W. Chen, F. Feng and Y. Jia, [arXiv:2312.17228 [hep-ph]]
- [29] H. n. Li, Y. L. Shen and Y. M. Wang, Phys. Rev. D **85**, 074004 (2012)
- [30] S. Cheng, Y. Y. Fan, X. Yu, C. D. Lü and Z. J. Xiao, Phys. Rev. D **89**, no.9, 094004 (2014)
- [31] P. Ball and R. Zwicky, Phys. Rev. D **71**, 014015 (2005)
- [32] P. Ball and R. Zwicky, Phys. Rev. D **71**, 014029 (2005)
- [33] C. Hambrock, A. Khodjamirian and A. Rusov, Phys. Rev. D **92**, no.7, 074020 (2015)
- [34] J. Chai and S. Cheng, [arXiv:2412.05941 [hep-ph]]
- [35] H. n. Li and S. Mishima, Phys. Rev. D **80** (2009), 074024
- [36] G.P. Lepage, S.J. Brodsky, T. Huang and P.B. Mackenzie, Banff Summer Institute, Particles and Fields 2, eds. A.Z. Capri and A.N. Kamal (1983) p.83
- [37] R. Jakob and P. Kroll, Phys. Lett. B **315** (1993), 463-470 [erratum: Phys. Lett. B **319** (1993), 545]
- [38] G.P. Lepage, S.J. Brodsky, T. Huang and P.B. Mackenzie, Banff Summer Institute, Particles and Fields 2, eds. A.Z. Capri and A.N. Kamal (1983) p. 83
- [39] S. Navas *et al.* [Particle Data Group], Phys. Rev. D **110**, no.3, 030001 (2024)
- [40] H. n. Li and G. F. Sterman, Nucl. Phys. B **381**, 129-140 (1992)
- [41] L. Chang, I. C. Cloët, C. D. Roberts, S. M. Schmidt and P. C. Tandy, Phys. Rev. Lett. **111** (2013) no.14, 141802
- [42] C. D. Roberts, D. G. Richards, T. Horn and L. Chang, Prog. Part. Nucl. Phys. **120** (2021), 103883
- [43] P. Jain, B. Kundu, H. n. Li, J. P. Ralston and J. Samuelsson, Nucl. Phys. A **666** (2000), 75-83
- [44] J. Chai, S. Cheng and J. Hua, Eur. Phys. J. C **83** (2023) no.7, 556
- [45] G. Wang *et al.* [ $\chi$ QCD], Phys. Rev. D **104** (2021), 074502
- [46] H. T. Ding, X. Gao, A. D. Hanlon, S. Mukherjee, P. Petreczky, Q. Shi, S. Syritsyn, R. Zhang and Y. Zhao, [arXiv:2404.04412 [hep-lat]]

- [47] J. P. Lees *et al.* [BaBar], Phys. Rev. D **86** (2012), 032013
- [48] M. Fujikawa *et al.* [Belle], Phys. Rev. D **78** (2008), 072006
- [49] M. Ablikim *et al.* [BESIII], Phys. Lett. B **753** (2016), 629-638 [erratum: Phys. Lett. B **812** (2021), 135982]
- [50] S. R. Amendolia *et al.* [NA7], Nucl. Phys. B **277** (1986), 168
- [51] T. Horn *et al.* [Jefferson Lab F(pi)-2], Phys. Rev. Lett. **97** (2006), 192001
- [52] G. M. Huber *et al.* [Jefferson Lab], Phys. Rev. C **78** (2008), 045203
- [53] J. Dudek, R. Ent, R. Essig, K. S. Kumar, C. Meyer, R. D. McKeown, Z. E. Meziani, G. A. Miller, M. Pennington and D. Richards, *et al.* Eur. Phys. J. A **48**, 187 (2012)
- [54] S. Cheng and Q. Qin, Phys. Rev. D **99**, no.1, 016019 (2019)
- [55] J. Hua *et al.* [Lattice Parton], Phys. Rev. Lett. **129** (2022) no.13, 132001
- [56] B. Delcourt, D. Bisello, J. C. Bizot, J. Buon, A. Cordier and F. Mane, Phys. Lett. B **99**, 257-260 (1981)
- [57] F. Mane, D. Bisello, J. C. Bizot, J. Buon, A. Cordier and B. Delcourt, Phys. Lett. B **99**, 261-264 (1981)
- [58] D. Bisello *et al.* [DM2], Z. Phys. C **39**, 13 (1988)
- [59] P. M. Ivanov, L. M. Kurdadze, M. Y. Lelchuk, V. A. Sidorov, A. N. Skrinsky, A. G. Chilingarov, Y. M. Shatunov, B. A. Shvarts and S. I. Eidelman, Phys. Lett. B **107**, 297-300 (1981)
- [60] P. m. Ivanov, L. m. Kurdadze, M. y. Lelchuk, E. v. Pakhtusova, V. a. Sidorov, A. n. Skrinsky, A. g. Chilingarov, Y. m. Shatunov, B. a. Shvarts and S. i. Eidelman, JETP Lett. **36**, 112-115 (1982)
- [61] M. N. Achasov, K. I. Beloborodov, A. V. Berdyugin, *et al.* Phys. Rev. D **63**, 072002 (2001)
- [62] M. N. Achasov, K. I. Beloborodov, A. V. Berdyugin, *et al.* Phys. Rev. D **76**, 072012 (2007)
- [63] R. R. Akhmetshin *et al.* [CMD-2], Phys. Lett. B **669**, 217-222 (2008)
- [64] T. K. Pedlar *et al.* [CLEO], Phys. Rev. Lett. **95**, 261803 (2005)
- [65] K. K. Seth, S. Dobbs, Z. Metreveli, A. Tomaradze, T. Xiao and G. Bonvicini, Phys. Rev. Lett. **110**, no.2, 022002 (2013)
- [66] J. P. Lees *et al.* [BaBar], Phys. Rev. D **88** (2013) no.3, 032013
- [67] J. P. Lees *et al.* [BaBar], Phys. Rev. D **92** (2015) no.7, 072008
- [68] M. Ablikim *et al.* [BESIII], Phys. Rev. D **99** (2019) no.3, 032001
- [69] G. J. Gounaris and J. J. Sakurai, Phys. Rev. Lett. **21**, 244-247 (1968)
- [70] J. H. Kuhn and A. Santamaria, Z. Phys. C **48**, 445-452 (1990)
- [71] H. Leutwyler, Phys. Lett. B **378**, 313-318 (1996)

- [72] J. Koponen, A. C. Zimmermann-Santos, C. T. H. Davies, G. P. Lepage and A. T. Lytle, Phys. Rev. D **96** (2017) no.5, 054501
- [73] Z. Q. Yao, D. Binosi and C. D. Roberts, Phys. Lett. B **855**, 138823 (2024)
- [74] L. B. Chen, W. Chen, F. Feng and Y. Jia, [arXiv:2407.21120 [hep-ph]]
- [75] H. J. Behrend *et al.* [CELLO], Z. Phys. C **49** (1991), 401-410
- [76] L. G. Landsberg, Phys. Rept. **128**, 301-376 (1985)
- [77] S. J. Brodsky and G. P. Lepage, Phys. Rev. D **24**, 1808 (1981)
- [78] J. Gronberg *et al.* [CLEO], Phys. Rev. D **57** (1998), 33-54
- [79] S. L. Adler, Phys. Rev. **177**, 2426-2438 (1969)
- [80] D. Melikhov and B. Stech, Phys. Rev. D **85**, 051901 (2012)
- [81] V. L. Chernyak and A. R. Zhitnitsky, Phys. Rept. **112**, 173 (1984)
- [82] F. G. Cao, T. Huang and B. Q. Ma, Phys. Rev. D **53**, 6582-6585 (1996)
- [83] P. Kroll and M. Raulfs, Phys. Lett. B **387**, 848-854 (1996)
- [84] T. Feldmann and P. Kroll, Eur. Phys. J. C **5** (1998), 327-335
- [85] I. V. Musatov and A. V. Radyushkin, Phys. Rev. D **56**, 2713-2735 (1997)
- [86] A. Khodjamirian, Eur. Phys. J. C **6**, 477-484 (1999)
- [87] A. Schmedding and O. I. Yakovlev, Phys. Rev. D **62**, 116002 (2000)
- [88] A. P. Bakulev, S. V. Mikhailov and N. G. Stefanis, Phys. Rev. D **67**, 074012 (2003)
- [89] S. S. Agaev, Phys. Rev. D **72**, 114010 (2005)
- [90] B. Aubert *et al.* [BaBar], Phys. Rev. D **80** (2009), 052002.
- [91] A. V. Radyushkin, Phys. Rev. D **80**, 094009 (2009)
- [92] M. V. Polyakov, JETP Lett. **90**, 228-231 (2009)
- [93] N. G. Stefanis, W. Schroers and H. C. Kim, Phys. Lett. B **449**, 299-305 (1999)
- [94] S. Nandi and H. n. Li, Phys. Rev. D **76**, 034008 (2007)
- [95] S. S. Agaev, V. M. Braun, N. Offen and F. A. Porkert, Phys. Rev. D **83**, 054020 (2011)
- [96] S. Uehara *et al.* [Belle], Phys. Rev. D **86** (2012), 092007
- [97] S. S. Agaev, V. M. Braun, N. Offen and F. A. Porkert, Phys. Rev. D **86**, 077504 (2012)
- [98] C. F. Redmer [BESIII], [arXiv:1810.00654 [hep-ex]]
- [99] B. Aubert *et al.* [BaBar], Phys. Rev. D **74** (2006), 012002
- [100] P. del Amo Sanchez *et al.* [BaBar], Phys. Rev. D **84** (2011), 05200
- [101] A. P. Bakulev, S. V. Mikhailov and N. G. Stefanis, Phys. Lett. B **508**, 279-289 (2001)
- [102] P. Kroll, "The form factors for the photon to pseudoscalar meson transitions - an update," Eur. Phys. J. C **71** (2011), 1623



- [103] S. S. Agaev, V. M. Braun, N. Offen, F. A. Porkert and A. Schäfer, Phys. Rev. D **90** (2014) no.7, 074019
- [104] A. Ali and A. Y. Parkhomenko, Phys. Rev. D **65**, 074020 (2002)
- [105] P. Kroll and K. Passek-Kumericki, J. Phys. G **40** (2013), 075005
- [106] S. S. Agaev and N. G. Stefanis, Phys. Rev. D **70**, 054020 (2004)
- [107] J. P. Lees *et al.* [BaBar], Phys. Rev. D **98** (2018) no.11, 112002
- [108] Y. Ji and A. Vladimirov, Eur. Phys. J. C **79** (2019) no.4, 319
- [109] H. Leutwyler, Nucl. Phys. B Proc. Suppl. **64**, 223-231 (1998)
- [110] E. Witten, Nucl. Phys. B **149**, 285-320 (1979)
- [111] T. Feldmann, P. Kroll and B. Stech, Phys. Rev. D **58** (1998), 114006
- [112] R. Escribano and J. M. Frere, JHEP **06** (2005), 029
- [113] R. Escribano, P. Masjuan and P. Sanchez-Puertas, Phys. Rev. D **89**, no.3, 034014 (2014)
- [114] F. G. Cao, Phys. Rev. D **85** (2012), 057501
- [115] G. S. Bali *et al.* [RQCD], JHEP **08**, 137 (2021)
- [116] D. Hatton *et al.* [HPQCD], Phys. Rev. D **102**, no.5, 054511 (2020)
- [117] G. S. Bali *et al.* [RQCD], JHEP **08**, 065 (2019)
- [118] V. M. Braun, G. P. Korchemsky and D. Müller, Prog. Part. Nucl. Phys. **51** (2003), 311-398
- [119] I. I. Balitsky and V. M. Braun, Nucl. Phys. B **311** (1989), 541-584
- [120] P. Ball, V. M. Braun and A. Lenz, JHEP **0605**, 004 (2006)
- [121] P. Ball, JHEP **9901**, 010 (1999)
- [122] J. P. Lees *et al.* [BaBar], Phys. Rev. D **81**, 052010 (2010)
- [123] H. Y. Cheng, H. n. Li and K. F. Liu, Phys. Rev. D **79** (2009), 014024
- [124] Y. D. Tsai, H. n. Li and Q. Zhao, Phys. Rev. D **85** (2012), 034002
- [125] A. Khodjamirian, C. Klein, T. Mannel and N. Offen, Phys. Rev. D **80**, 114005 (2009)